Windfarm initiated Nature development with Native Oyster Reefs (WINOR)

WP2:

Developing efficient approaches for tracking the fate of loosely deployed flat oysters

Zhiyuan Zhao, Lennart van IJzerloo, Jan van Poppel, Tjeerd, J. Bouma

Final report

2023.12.13

Royal Netherlands Institute for Sea Research

Contents

Summary

Background: European flat oyster (*Ostrea edulis*) reefs are keystone habitats within the North Sea ecosystem, playing a vital role in bolstering biodiversity. Nevertheless, their distribution range underwent a severe contraction about a century ago due to diseases, pollution, harsh winter conditions, and overfishing, leading to functional extinction in certain regions. Consequently, extensive efforts have been undertaken to restore these oyster reefs in the North Sea. In most restoration pilots, the introduction of initial populations was accompanied by enhancement measures, such as deploying weighted cages containing live flat oysters and installing flat oyster tables, to prevent losses and provide a settling substrate for the generated larvae. While these measures can promote flat oyster restoration and enhance local biodiversity, their implementation is complex and costly, limiting the scaling-up of flat oyster restoration. Against this background, an ambitious restoration pilot has been implemented at the Gemini wind farm since 2021, in which flat oysters were loosely deployed on the seafloor to kick-start self-sustaining populations with minimal human intervention. With it comes uncertainty about the fate of the loosely deployed flat oysters.

Objectives: In the WINOR project, we were committed to developing and testing innovative monitoring technologies to uncover the fate of loosely deployed flat oysters within the Gemini wind farm, with the following specific research objectives:

i. Identifying the key environmental conditions under which flat oysters feed to maintain healthy growth.
ii. Quantifying the critical hydrodynamic conditions that result in the dislodgement of loosely deployed flat oysters (i.e., the critical dislodgement threshold).
iii. Tracking the position changes of loosely deployed flat oysters to reproduce their potential movements.

Methods: The following specific monitoring approaches were tailored in alignment with our research objectives. All of them were tested and evaluated during the restoration practices conducted within the Gemini wind farm.

- **Biophys sensor:** This sensor enables long-term, high-frequency, in-situ measurements of valve opening and closing in live oysters, making it an effective method for monitoring feeding behavior and health. Biophys sensors with live flat oysters attached were deployed twice within the Gimini wind farm during the winters of 2021-2022 and 2022-2023. Combined with simultaneous measurements of environmental parameters, it provided valuable insights into the reasons for the suitability or unsuitability of the target site.
- **Biophy-logging package:** This package comprises flat oyster mimics equipped with accelerometers and a wave radar. Specifically, accelerometers were embedded in flat oyster shells to achieve long-term, high-frequency, in-situ monitoring of the stability of loosely deployed flat oysters (mimics). By integrating the high-frequency wave data obtained by the wave radar, this package enables the quantification of critical hydrodynamic thresholds that induce the dislodgement of loosely deployed flat oysters. The monitoring campaign was conducted once at the Gemini wind farm during the winter of 2022-2023.
- **Acoustic telemetry array:** This monitoring system relies on the detection of underwater acoustic signals to pinpoint the positions of loosely deployed flat oysters, enabling the reproduction of their long-term activity trajectories and ranges. Deployment of this system was synchronized with the restoration efforts conducted within the Gemini wind farm during the winter of 2022-2023, ensuring that flat oysters with acoustic tags settled within the array.

Main results: The following results concerning the fate of loosely deployed flat oysters were derived from the data obtained using the above monitoring methods:

1. The conditions within the Gemini wind farm meet the requirements for the healthy growth of flat oysters. Temperature and salinity were identified as key factors and can be used as indicators to infer the habitat suitability regarding flat oyster feeding.

2. The critical dislodgement threshold (with near-bed orbital velocity as a quantitative index) of loosely deployed flat oysters (mimics) within the Gemini wind farm was determined to be 0.52 m s^{-1}.
3. The residency of loosely deployed flat oyster individuals and clusters within the Gemini wind farm was extremely low, without significantly different between them. Specifically, both individuals and clusters exhibited slow movement within a small spatial dimension in the first month after deployment, with weight playing a more significant role than near-bed orbital velocity. However, after certain dates characterized by strong near-bed orbital velocity (mainly occurring in January 2023), it is highly likely that all the deployed flat oyster individuals and clusters were expelled from the initial deployment site and did not return.
4. The flat oyster individuals and clusters deployed within the Gemini wind farm were at a high risk of being buried, considering the relative sediment accretion height of up to 10 cm in the area near the study site during monitoring period. This may be one reason for the short-term loss of acoustic signals during the residence of flat oysters (both individuals and clusters) within the acoustic telemetry array. However, the permanent loss of acoustic signals should be attributed to strong waves, because: 1) the acoustic signals were no long be detected even though the bed level returned to their initial state following the occurrence of erosion; 2) the near-bed orbital velocity corresponding to the expulsion of all deployed flat oyster individuals and clusters from the acoustic telemetry array aligned with the critical dislodgement threshold quantified using the Biophy-logging package.

Conclusions: The novel technologies developed in the WINOR project, including the Biophy-logging package and acoustic telemetry array, are suitable for determining *i*) the critical dislodgement threshold and *ii*) the fate of loosely deployed flat oyster individuals and clusters. Combining these newly developed technologies with the existing Biophys sensor that measures valve-gaping and ASED sensor measuring bed-level changes, this offers an effective approach to assess habitat suitability before restoration and track flat oyster fate during restoration.

Hydrodynamically-induced dislodgement, rather than feeding constraints related to water quality, constitutes the primary bottleneck in restoration efforts involving the loose deployment of

flat oyster individuals and clusters. Priority should, therefore, be given to comparing the hydrodynamic regimes of target sites with the critical dislodgement threshold of flat oysters (both individuals and clusters) during habitat suitability assessments. A potential strategy to minimize loss is to locate relatively hydrodynamically sheltered sites (e.g., channels between ridges) and deploy the initial populations there. Otherwise, artificial shelters need to be added to enhance the stability of the initial population under hydrodynamic disturbance.

Derived knowledge gaps: Open questions resulting from the WINOR project include but are not limited to the following:

- Are the dislodged flat oysters aggregating at new locations with a sufficient density to serve as a starting point/nursery for reef development?

The deployed flat oysters were dislodged upon the critical hydrodynamic threshold being exceeded, indicating the possibility of them staying in a group at new locations. Using remotely operated vehicles (ROV) to search around the initial deployment location may be one potential approach to unraveling this puzzle. Nevertheless, it is recommended to engage in collaborations with other projects utilizing ROV for seabed scanning, as this task is comparable to finding a needle in a haystack and involves substantial costs.

- To what extent do the magnitude and frequency of sediment (or shell material) burial affect the performance of flat oysters?

Multiple storms occurred during the winter of 2021-2022, resulting in a cumulative sediment accretion of up to 25 cm within the study area. Although there were no storms during the winter of 2022-2023, shallower sediment accretion (less than 10 cm) lasting for one month was detected. This suggests that flat oysters deployed within the Gemini wind farm face the risk of being buried, but the extent to which sediment burial impacts flat oyster performance remains to be rigorously verified.

1. General introduction

Flat oyster (*Ostrea edulis*), an endemic species of the European marine environment, can form extended biogenic reefs with a large influence on the ecosystem (Kamermans et al., 2018). Specifically, the flat oyster reefs can promote a more stable seabed compared to open sandy/muddy seabed by reducing turbulence and consolidating sediment (Housego & Rosman, 2016). Their intricate and robust substrate structure provides habitat, food, shelter, and spawning/nursery grounds for many associated species (Plunket & La Peyre, 2005; Crawford et al., 2019). Additionally, the presence of oyster reefs contributes to enhanced water quality by filtering and sequestering suspended organic and inorganic particles in (pseudo) feces (Kreeger et al., 2018). In essence, the habitats they create often serve as hotspots for marine biodiversity.

The flat oysters are native to the northeastern Atlantic Ocean and were once widely distributed along the coastlines of Europe, from the Scandinavian Peninsula to the Black Sea, as well as in deeper offshore waters (Bennema et al., 2020; Merk et al., 2020). In Dutch marine waters, substantial biogenic reefs formed by flat oysters were once found in the Dutch Wadden Sea, the northern parts of the former Zuiderzee, and offshore in the North Sea (Kamermans et al., 2018). However, by the late 19th and early 20th centuries, a range of adverse factors, including overexploitation in bottom trawling fisheries, the introduction of non-native oysters, climate change, and outbreaks of specific diseases, had led to a critically low population of wild flat oyster reefs in the United Kingdom, Ireland, France, the Netherlands, Denmark, Portugal, and Spain (Gercken & Schmidt, 2014; Bennema et al., 2020; Merk et a., 2020). In Germany and the Belgian North Sea, flat oyster reefs have become functionally extinct (Pogoda, 2019; Merk et a., 2020). Nowadays, a few scattered flat oyster reefs are found only in estuarine environments in the Netherlands, ranging from 0 to 6 meters in depth, primarily in the form of mixed reefs with *Magellana giga*s and as offspring of aquaculture (Sas et al., 2023). Overall, the loss of flat oyster reefs has been so extensive that active restoration measures are required.

The Dutch government is therefore aiming to enhance and/or restore flat oyster reefs in the North Sea where feasible. An initial step is to eliminate the primary threat to the persistence of flat oyster reefs in specific areas, which is achieved by legislating against bottom trawling and other forms of seabed disturbance (Fowler et al., 2020). This ban came into effect primarily on March 8, 2023, with the affected areas accounting for 5% of the Dutch North Sea's exclusive economic zone

and projected to expand to 15% by 2030 (OFL, 2020). Furthermore, the construction of offshore wind farms has resulted in an increasing number of areas in the Dutch North Sea being protected from anthropogenic seabed disturbances (Kamermans et al., 2018). Practical research conducted in recent years has identified offshore wind farms as the most promising locations for flat oyster reef restoration (Didderen et al., 2019; van Duren et al., 2022; Bos et al., 2023a). This is because the turbine foundations can serve as artificial reefs for the settlement of free-swimming oyster larvae, and the areas between turbines prohibit bottom trawling, minimizing seabed disturbances (Smaal et al., 2015; Kamermans et al., 2018; Hermans et al., 2020). Flat oysters are now a focal species in nature-inclusive designs for offshore wind farms in the Netherlands (Hermans et al., 2020). In the future, the potential areas for flat oyster restoration are set to significantly expand, given the planned governmental expansion of nature protection zones and the scaling up of offshore wind energy in the Dutch North Sea.

Notably, flat oysters cannot naturally form coral reefs in the Dutch North Sea within the foreseeable future (Kerckhof et al., 2018; Sas et al., 2023). This is primarily due to the disappearance of flat oyster reefs in the region, resulting in a shortage of larvae and a lack of natural settlement substrate (i.e., oyster shells). As a result, restoring or creating flat oyster reefs requires the introduction of starting populations. The ongoing restoration pilots in the Dutch North Sea involve the translocation of adult oysters from Ireland, Norway, and the Netherlands (Didderen et al., 2019; van Duren et al., 2022). This underscores the need for evaluating the performance of these oysters from foreign sources in the early stages of restoration. Typically, this evaluation involves deploying the translocated oysters on the seabed in enclosed structures and periodically raising them to monitor their vitality and activity (Bos et al., 2023b; Pineda-Metz et al., 2023). Encouragingly, the assessment results from multiple restoration pilots suggest that the overall environmental conditions in the Dutch North Sea are still conducive for flat oysters, whether from foreign or local sources, to survive, grow, and reproduce (Bos et al., 2023a). In these restoration pilots, the introduction of starting populations is often accompanied by enhancement measures, such as deploying weighted cages with live oysters and installing oyster tables (structures made of concrete and other materials on which live oysters are placed), to prevent the loss of translocated oysters and provide settlement substrates for the generated larvae (Didderen et al., 2019; van Duren et al., 2022; Pineda-Metz et al., 2023). While these measures can promote oyster restoration and

enhance local biodiversity, they are complex to implement and come with high costs, thereby restricting the scaling-up of flat oyster reef restoration.

More importantly, restoration efforts should aim to minimize human intervention and allow nature to develop as naturally as possible. In other words, the ultimate restoration goal in the Dutch North Sea is to kick-start self-sustaining or autonomously growing flat oyster reefs (Sas et al., 2023). Two restoration projects in two wind farms, namely Borkum Reef Ground and Gemini, are currently being implemented for this purpose by deploying individual flat oysters on the seafloor (Didderen et al., 2020; Sas et al., 2023). In this context, the growth rate alone is not a comprehensive enough indicator to illustrate project performance. Such limitation arises from the potential impact of currents and wave-induced turbulence in the North Sea, which may lead to the dislodgment and dispersion of loosely deployed flat oysters, thus hindering the formation of biogenic reefs (Colden et al., 2016; Smaal et al., 2017). This speculation has been confirmed in the project conducted in the Borkum Reef Grounds wind farm, where 80,000 flat oysters were loosely deployed, with only a few being retraced in later monitoring (Sas et al., 2023). This outcome can be attributed to turbulence induced by regular storm events, as demonstrated in models and verified through basin experiments (Bos et al., 2023b). Nevertheless, the project conducted at the Gemini wind farm is considered more promising, as preliminary investigations indicated that the deeper water and lower wave impact on the seabed result in less seabed dynamics. In the winter of 2022, over 1,500 flat oysters and 18 tons of shell material were lowered onto the seabed of the Gemini wind farm, covering a total area of 5 hectares. In the summer of 2023, about 3,000 flat oysters, hundreds of thousands of baby oysters, and 48 tons of shell material were added. The immediate challenge is to employ efficient methods to monitor the stability of the loosely deployed flat oysters under local hydrodynamic regimes, i.e., determining whether they will remain in place or move through the wind farm.

Additionally, the overall understanding of the conditions suitable for the long-term development of offshore flat oyster reefs remains limited, since it is largely derived from historical information (when the reefs were still present; Stechele et al., 2023a, b). However, once the oyster reefs disappear, local conditions may no longer be conducive to the initiation and growth of new flat oyster reefs (Stechele et al., 2023a, b). Thus, there is an urgent need to pinpoint the current conditions required for the formation of offshore flat oyster reefs, including key environmental

factors that promote the healthy growth and long-term survival of individual flat oysters, ultimately leading to an enhancement of habitat suitability models that are currently reliant on historical data. Furthermore, a substantial portion of the North Sea seabed is composed of sandy and silty sediments, which may not provide an appropriate settling substrate for flat oysters and could become loose due to natural sand waves, potentially causing oysters to be overturned or buried (Luff & Moll et al., 2004). This has been confirmed in restoration pilots conducted in other locations, such as the partial burial of heavy deployment cages in Luchterduinen and the probable burial and scattering oysters over a large area in Borkum Reef Ground (Bos et al., 2023b; Sas et al., 2023). Therefore, even though the Gemini wind farm is known to have fewer seabed structures (such as sand waves and mega-ripples) than other areas in the North Sea, it is essential to assess local bed level dynamics, especially during storm events, to determine the likelihood of oysters being buried after deployment.

In this project, our focus is on the restoration practices conducted at the Gemini wind farm, where flat oysters were loosely deployed to initiate self-sustaining populations. By employing innovative research methods, we aim to achieve the following objectives:

1) Identifying the key environmental conditions under which flat oysters feed to maintain healthy growth.
2) Quantifying the critical hydrodynamic conditions that result in the dislodgement of loosely deployed flat oysters (i.e., the critical dislodgement threshold).
3) Tracking the position changes of loosely deployed flat oysters to reproduce their potential movements before being lost.

This project holds the potential not only to enhance our mechanistic understanding of flat oyster reef formation in offshore areas but also to improve existing predictive models. It will enable a more precise identification of the windows of opportunity for flat oysters to maintain their well-being and the windows of risk responsible for the dislodgement or even the collapse of restored flat oyster reefs. Consequently, this will increase the feasibility of large-scale offshore flat oyster restoration.

2. Identifying key factors influencing flat oyster feeding

2.1 Introduction

The health of flat oysters at target restoration sites is a crucial performance parameter in the restoration project (Baggett et al., 2015; Zu Ermgassen et al., 2021). The assessment of flat oyster health can be achieved by monitoring their key physiological functions, including feeding and respiration. In principle, wide-open valves indicate feeding and respiration, while partially closed or closed valves suggest reduced or halted filtration (Bertolini et al., 2022). Monitoring these parameters is often challenging given the remote offshore locations, and innovative techniques are required to reduce the frequency of access to these sites. In this section, we utilized Biophys sensors developed by NIOZ to monitor the performance of flat oysters at the restoration site (i.e., the Gemini windfarm) and thus to achieve our research **objective-1:** ***Identifying the key environmental conditions under which flat oysters feed to maintain healthy growth***. These sensors enable the long-term, high-frequency, in-situ measurement of live oyster valve opening and closing, making it an effective method for monitoring feeding behavior and health. When combined with simultaneous measurements of environmental parameters such as temperature, salinity, flow velocity, and chlorophyll-a, it can provide valuable insights into the reasons for the suitability or unsuitability of the target site.

2.2 Methods

2.2.1 Biophys sensor

The Biophys sensor (Fig. 2.1a), developed by NIOZ, serves as a long-term autonomous data recording instrument used to measure valve-gaping of flat oysters. After attaching a small magnet to the oyster shell, the Biophys sensor can detect changes in Hall numbers based on a magnetism sensor (DRV5053VAQLPGM). These changes in Hall numbers can be further converted into the proportion of oyster valve openness (Fig. 2.1b). The magnet's size (Ø = 3 millimeters) is chosen to be as small as possible to minimize behavioral interference while still being large enough to emit a signal distinguishable from the Earth's magnetic field. The Biophys sensor can also simultaneously measure water pressure and temperature using a pressure sensor

(MS580314BA01) and a temperature sensor (TSIC506F). All sensors are located in the head of the Biophys sensor. The minimum sampling frequency is 0.1 second. During field monitoring, the sampling frequency for all parameters was set to 1 second to avoid unnecessary battery usage while still obtaining high-frequency samples.

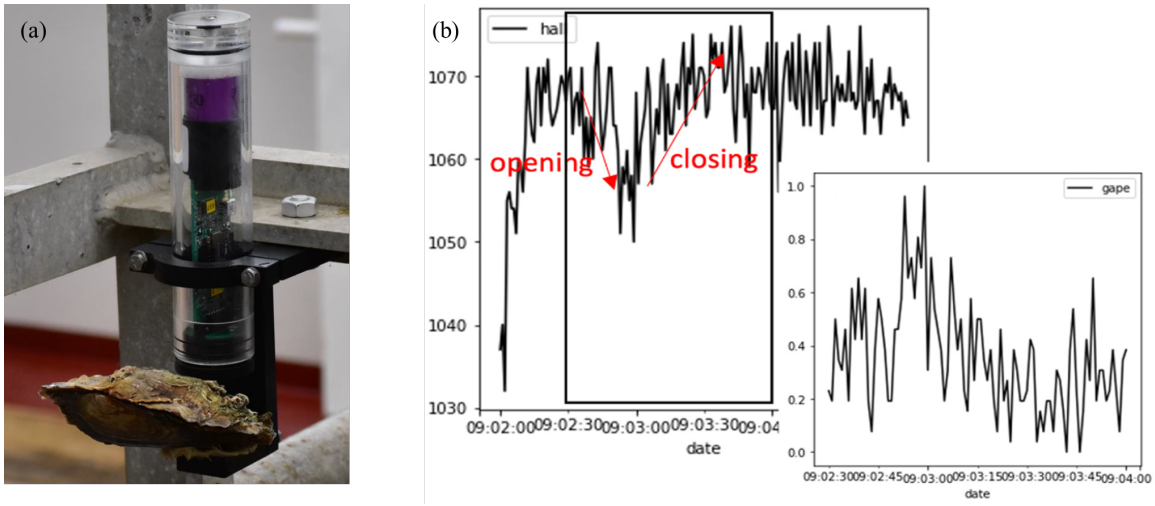

Fig. 2.1 (a) Photo of the Biophys sensor with a live flat oyster attached for testing. (b) Example of the data from the Biophys sensor. The flat oyster valve opens as the Hall number decreases and closes as the Hall number increases. The subplot in the bottom right shows the transformed data, with 1 indicating the oyster is fully open and 0 indicating the oyster is fully closed.

2.2.2 Field monitoring

Field monitoring related to oyster gaping activity was conducted twice, during the winters of 2021-2022 and 2022-2023, within the Gemini wind farm (Fig. 2.2a). In each monitoring campaign, ten Biophys sensors were deployed, with each one being configured with a live adult flat oyster at the time of deployment. These sensors were installed on custom-made metal frames named MIXLander (Fig. 2.2b) and submerged to a depth of approximately 32 meters on the seabed. Additionally, two ADCPs (one facing upward and one facing downward), four ASEDs, and one C3 sensor were mounted on the MIXLander to synchronize the monitoring of velocity profiles, seabed level changes, chlorophyll-a content, and turbidity at their respective minimum sampling frequencies. Unfortunately, the upward-facing ADCP and C3 sensors did not function properly during both monitoring campaigns, and the downward-facing ADCP worked for only a limited

period (approximately 12 days) due to battery constraints. Consequently, we utilized open-access datasets to meet our subsequent data analysis requirements, as detailed in Section 2.2.3.

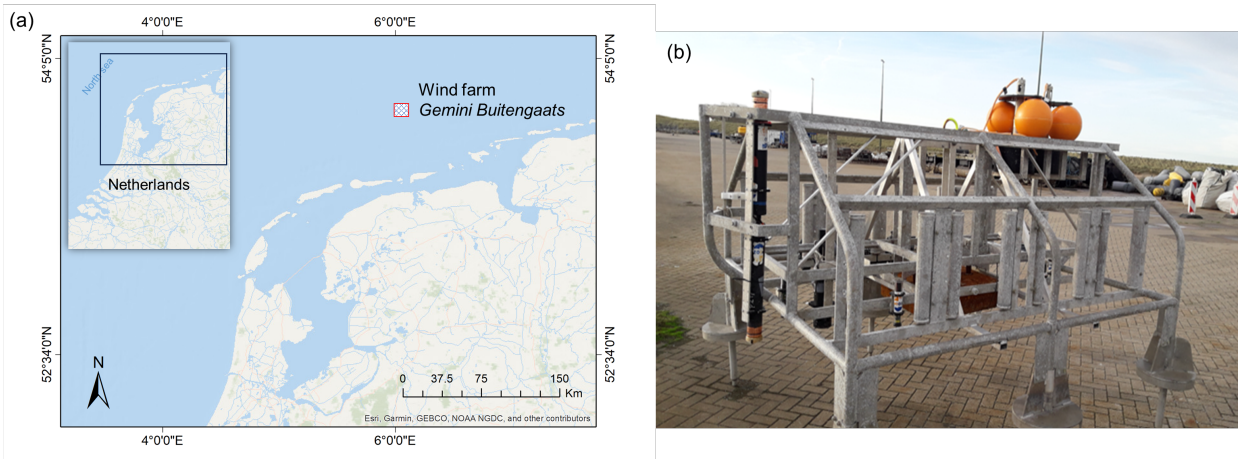

Fig. 2.2 (a) Geographical location of the Gemini wind farm. (b) Photo of the framework called MIXLander used to deploy multiple instruments including Biophys sensors, ADCP, ASED and C3 sensor.

2.2.3 Collection of environmental datasets

Water quality parameters considered include (1) ***salinity***, which has been demonstrated to affect the functionality of marine ecosystems; (2) ***chlorophyll-a*** *concentration* as an estimate of phytoplankton biomass, describing the approximate food availability; (3) ***dissolved oxygen***, as stratification can occur in North Sea regions, potentially leading to oxygen depletion and limiting habitat suitability; and (4) ***pH***, as decreased pH has been documented to have a negative impact on the growth rates of mollusks in multiple meta-analyses. Daily average model outputs for all the mentioned water quality parameters were extracted from the Atlantic-European Northwest Shelf-Ocean Biogeochemistry Reanalysis model (available at the Copernicus Marine Service's Data Portal: https://marine.copernicus.eu). This model provides the temporal evolution of each variable at a depth of 30 meters below the sea surface.

The Biophys sensor measured the (5) ***temperature*** at a depth of approximately 32 meters with a sampling frequency of 1 Hz. Daily averages were computed to obtain manageable time series data for comparison with other environmental variables.

Wave data characterizing the hydrodynamic conditions at the research site was obtained from a wave radar located within the Gemini windfarm. Significant wave height was converted to (6) ***near-bed orbital velocity*** using the method described in Section 4.2.3. Daily averages were used to generate manageable time series data for comparison with other environmental variables.

It's worth noting that, while data regarding temperature and near-bed velocity are available for both monitoring campaigns, open-access data regarding water quality (including salinity, dissolved oxygen, chlorophyll-a, and pH) is only accessible for the winter of 2021-2022. The relevant data for the winter of 2022-2023 remains currently unavailable, due to the time lag in open-access modeling data. Note, bed-level changes were not considered here because the flat oysters used for monitoring were fixed on the Biophys sensors, about 0.5 m away from the bed, making them insulated from the effects of bed-level changes. However, this data was later used to explain the movement of loosely deployed flat oysters (see Section-4 and Section-5).

2.2.4 Data analysis

2.2.4.1 Identifying patterns in flat oyster gaping activity

The Biophys sensor detects oyster gaping activity, i.e., the opening and closing of oyster shells, by monitoring changes in Hall numbers at a frequency of 1 Hz. To mitigate the influence of noise spikes (which are rare but do exist) on oyster gaping calculations, outliers were removed based on the lower and upper quantiles (5^{th} and 95^{th} percentiles). To ensure comparability of results across individuals and time periods, the relative proportion of valve opening (0 represents complete closure, and 1 represents full opening; Fig. 2.1b) for each individual was calculated using the following formula:

$$Gape = \frac{\text{abs}(\text{hall} - \max(\text{hall}))}{\max(\text{hall}) - \min(hall)}$$

Where $Gape$ is the proportion of valve opening, and $hall$ is the Hall numbers recorded by Biophys sensors. Averages over 5-minute intervals were calculated to obtain manageable time series.

To identify potential patterns in flat oyster gaping activity, an unsupervised machine learning method, namely k-means clustering, was applied to the overall gape time series. The

optimal number of clusters was determined using both the elbow method, selecting the cluster number that optimizes both ‘within’ and ‘between’ sums of squares, and visually examining the resulting principal component plot to prevent excessive overlap between groups.

2.2.4.2 Linking flat oyster gaping patterns with environment

To explore whether the average proportion of valve opening was influenced by environmental conditions, the k-means clustering algorithm was applied to the daily averages of oyster gaping and available environmental variables (i.e., temperature, salinity, dissolved oxygen, chlorophyll-a, pH, and near-bed orbital velocity). All environmental variables were standardized within the range of 0 (minimum) to 1 (maximum). This analysis was conducted solely using data collected during the winter of 2021-2022, as open-access data related to water quality (including salinity, dissolved oxygen, chlorophyll-a, and pH) for the winter of 2022-2023 are currently unavailable.

As further data exploration, pairwise correlation analysis was employed to detect potential associations among the key environmental variables identified by the clustering algorithm. Variables with a correlation coefficient $|\rho| > 0.6$ were considered autocorrelated and filtered to retain one of them. To accomplish this, one of the autocorrelated variables was modeled against oyster gaping using the generalized linear model. Variables corresponding to candidate models with a higher AIC (Akaike Information Criterion) were eliminated. Subsequently, the daily averages of oyster gaping and the remaining environmental variables were used to construct Random Forest regression models. This was done to: 1) rank the importance of the key environmental variables identified by the clustering algorithm, and 2) determine the optimal number of key environmental variables for accurately predicting flat oyster gaping activity. The latter was achieved by modeling with all the environmental variables identified by the clustering algorithm and modeling with the reduced environmental variables, followed by comparing model performance. Finally, the relationship between flat oyster gaping and the remaining key environmental variables was established.

2.3 Results

2.3.1 Patterns in flat oyster gaping activity

Based on unsupervised machine learning using the overall gaping time series (with 5-minute intervals), a similar gaping pattern was observed for oysters tested in the two monitoring campaigns (Fig. 2.3). Overall, the optimal number of clusters for oyster gaping activities is 3, corresponding to wider, moderate, and narrower gaping angles, with their differences primarily related to daily average gaping. Specifically, for oysters monitored during the winter of 2021-2022, the clusters were separated along an axis that explained 89.6% of the variability, with wider (average 70%), moderate (49%), and narrower (33%) gaping angles (Fig. 2.3a). For oysters monitored during the winter of 2022-2023, the clusters were separated along an axis that explained 67.5% of the variability, with wider (average 68%), moderate (46%), and narrower (25%) gaping angles (Fig. 2.3b). The slight differences in flat oyster gaping patterns between the two monitoring campaigns may be attributed to 1) differences in the status of flat oysters used, including their origin, age, and size; 2) variations in environmental conditions between years (see section 2.3.2 for the impact of environment on oyster gaping).

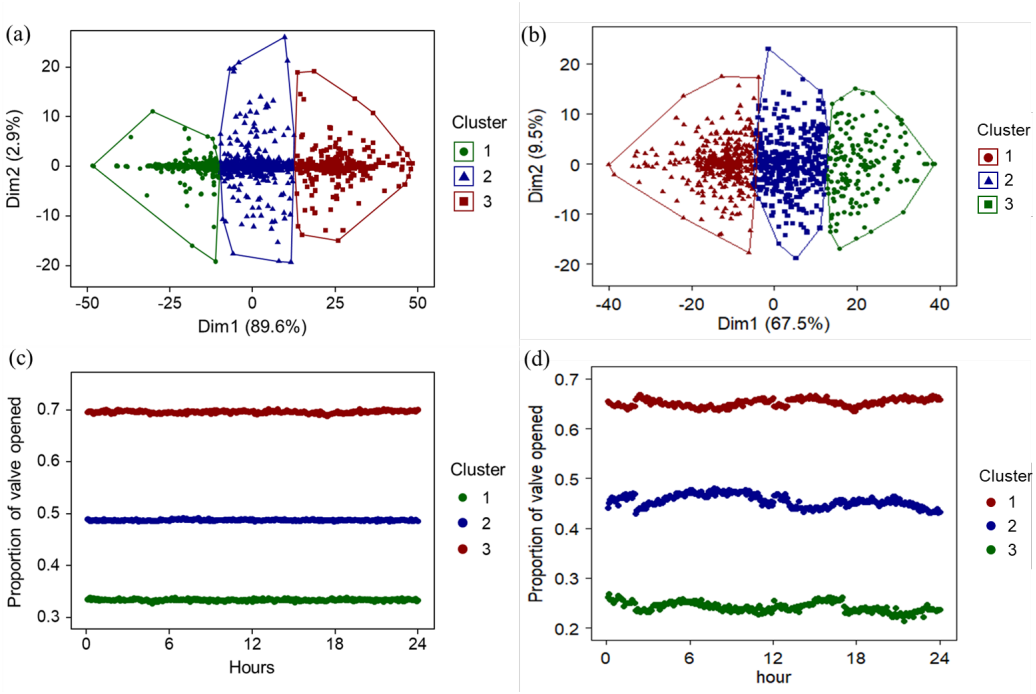

Fig. 2.3 Principal component representation of k-means clustering of daily gaping curves (a, b) and the pattern of gaping for each cluster centroid (c, d). Regarding time, a and c refer to the gaping

data collected during the winter of 2021-2022, while b and d represent gaping data collected during the winter of 2022-2023. The colors of each cluster in the principal component representation match the colors of their pattern representation.

2.3.2 Oyster gaping vs environmental variables

This section presents results based on field monitoring conducted during the winter of 2021-2022, as data for water quality parameters in the winter of 2022-2023 is unavailable.

2.3.2.1 Environmental conditions

During the field monitoring conducted in the winter of 2021-2022: (1) ***Temperature***: The daily average water temperature exhibited a trend of initial decrease followed by an increase, with a range of 6-13°C (Fig. 2.4). The coldest month was March, with an average temperature of 7°C. (2) ***Salinity***: The overall fluctuations in daily average salinity were small, ranging from 32.5 to 34.5. A slight increase of approximately 0.5 occurred in late January, followed by a noticeable decrease since March (from 34.5 to 33.0; Fig. 2.4). (3) ***Dissolved oxygen***: The overall trend of daily average dissolved oxygen content showed an increase, ranging from 230 to 290 mmol m^{-3} (Fig. 2.4), although a slight decrease occurred at the end of the monitoring period (May). (4) ***Chlorophyll-a***: The daily average chlorophyll content exhibited a decreasing trend in the early stages of monitoring (from 0.6 to 0.1 mg m^{-3}). Starting in mid-January, the daily average chlorophyll content began to rise and reached its peak in February (1.1 mg m^{-3}), remaining relatively stable with small fluctuations until the end of the monitoring. (5) ***pH***: The daily average pH remained relatively stable throughout the monitoring period, with slight fluctuations within the range of 8.02 to 8.08 (Fig. 2.4). (6) ***Near-bed orbital velocity***: Multiple storm events occurred during the monitoring period, with the minimum daily average near-bed orbital velocity being 0.5 m s^{-1} and reaching up to 0.8 m s^{-1} (Fig. 2.4). On calm days without storms, the daily average near-bed orbital velocity remained below 0.25 m s^{-1}. Especially after March, the near-bed orbital velocity was lower than 0.1 m s^{-1} on most days (Fig. 2.4). It is worth noting that the occurrence of storm events seemed to only affect the near-bed orbital velocity significantly at the monitoring site

and did not cause obvious fluctuations in other considered environmental variables, including temperature, salinity, dissolved oxygen, chlorophyll-a, and pH.

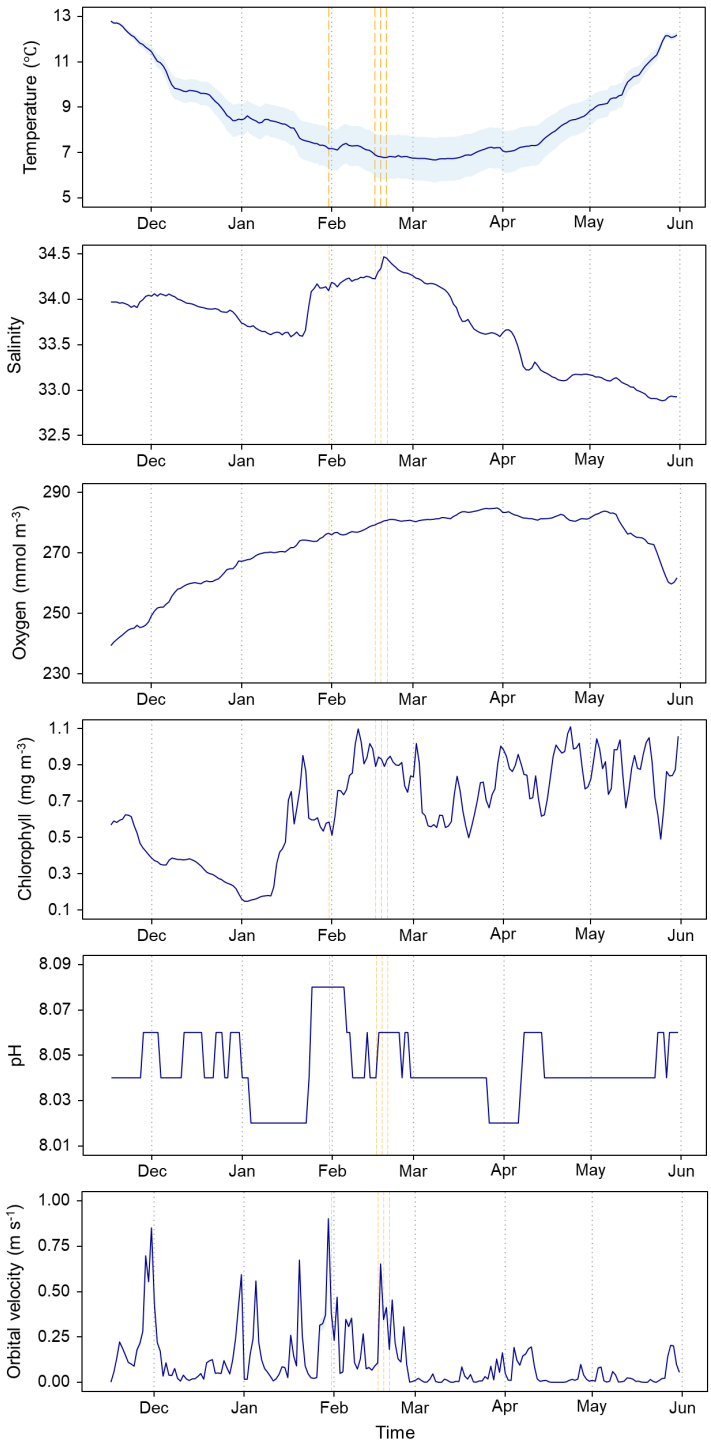

Fig. 2.4 Environmental conditions during the period of field monitoring at the winter of 2021-2022, including temperature, salinity, dissolved oxygen content, chlorophyll-a content, pH, and

near-bed orbital velocity. All data are presented as daily averages. The dashed orange lines indicate the dates of storms, including *Corrie* (January 31, 2022), *Dudley* (February 16, 2022), *Eunice* (February 18, 2022), and *Franklin* (February 20, 2022).

2.3.2.2 Environmental factors driving flat oyster gaping

Daily averages of oyster gaping and environmental variables were clustered in the second unsupervised machine learning, with three new clusters being identified (Fig. 2.5a). Overall, days with wider daily oyster gaping were clustered with higher chlorophyll-a and dissolved oxygen concentrations, relatively higher temperatures, as well as lower salinity and near-bed orbital velocity (Fig. 2.5b). Conversely, occasions when flat oysters had narrower gaping were colder days with lower chlorophyll-a and dissolved oxygen concentrations, as well as higher salinity (Fig. 2.5b). There was no detectable association between flat oyster gaping patterns and pH.

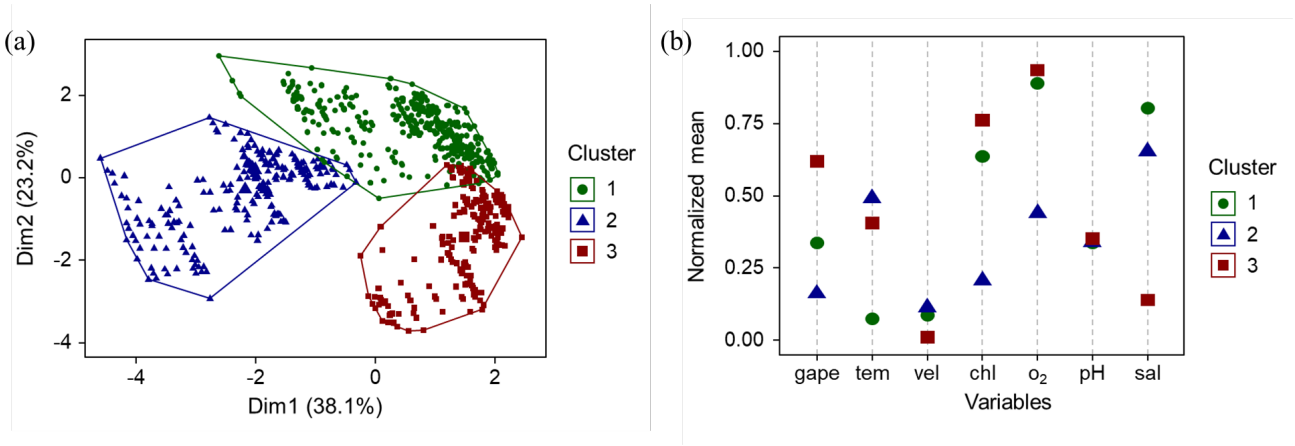

Fig. 2.5 (a) Principal component representation of k-means clustering of average daily gaping and rescaled environmental variables; (b) Values of average gaping and rescaled environmental variables (tem = temperature, vel = near-bed velocity, chl = chlorophyll-a, O_2 = dissolved oxygen, pH = pH, sal = salinity) for each cluster centroid.

In the subsequent variable selection procedures, dissolved oxygen content was eliminated from the candidates for key variables because it showed significant autocorrelation with temperature (Fig. 2.6) and performed poorly in the comparison using generalized linear models.

The developed random forest regression model (Fig. 2.7) indicated the relative importance of the remaining variables in regulating flat oyster gaping, with salinity being the most important variable, followed by temperature and chlorophyll-a concentration, while near-bed orbital velocity was comparatively less important (Fig. 2.8a). After modeling with different numbers of candidate variables and comparing model performance, it was found that a random forest model constructed using only two variables performed best in predicting flat oyster gaping (Fig. 2.8b). These two variables were ultimately identified as the key environmental factors governing flat oyster gaping, corresponding to the top two variables in terms of importance, namely salinity and temperature (Fig. 2.8a). The 3D response surface of flat oyster gaping to these two key factors exhibited results similar to those obtained from cluster analysis, that is, flat oysters tend to open wider (i.e., feed more) on relatively warm and low-salinity days (Fig. 2.9).

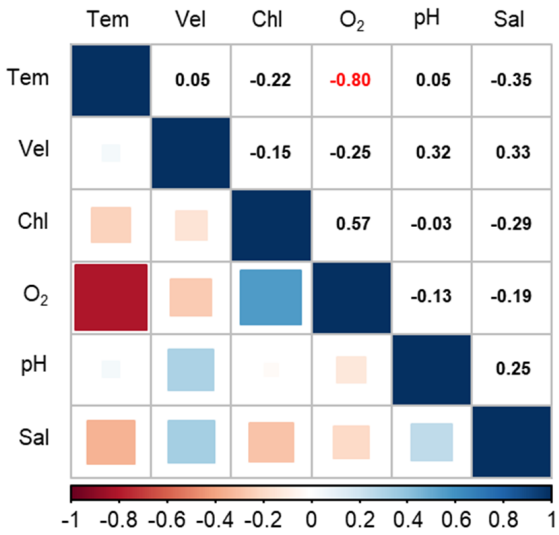

Fig. 2.6 Correlation of environmental variables (tem = temperature, vel = near-bed velocity, chl = chlorophyll-a, O_2 = dissolved oxygen, pH = pH, sal = salinity). Pairwise variables with an absolute correlation coefficient greater than 0.6 are considered to be autocorrelated (highlighted in red)

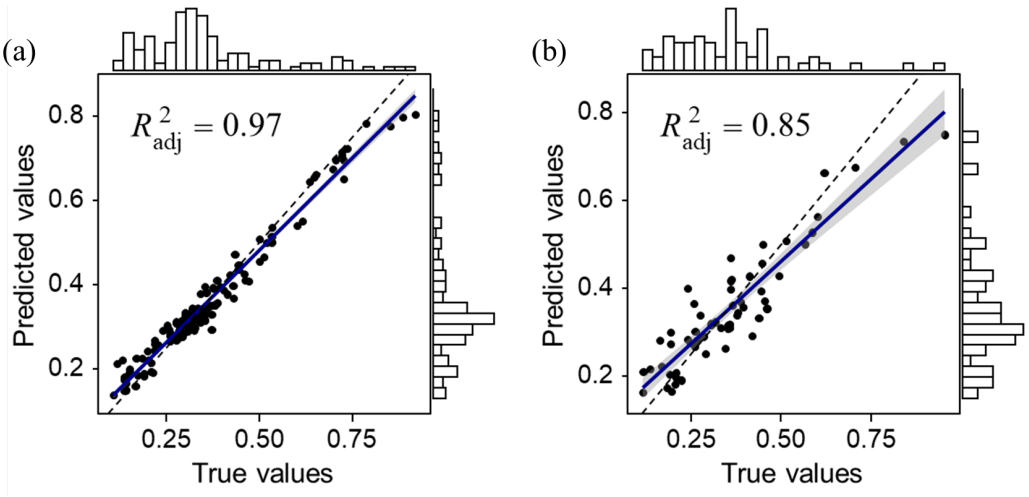

Fig. 2.7 Performance of the random forest model assessed using test subset (a) and validation subset (b). The true values are oyster gaping recorded by the Biophys sensors, and the predicted values are oyster gaping predicted by the random forest using the corresponding environmental data. This model was then used to rank the relative importance of environmental variables in dominating flat oyster gaping, refer to Fig. 2.8a.

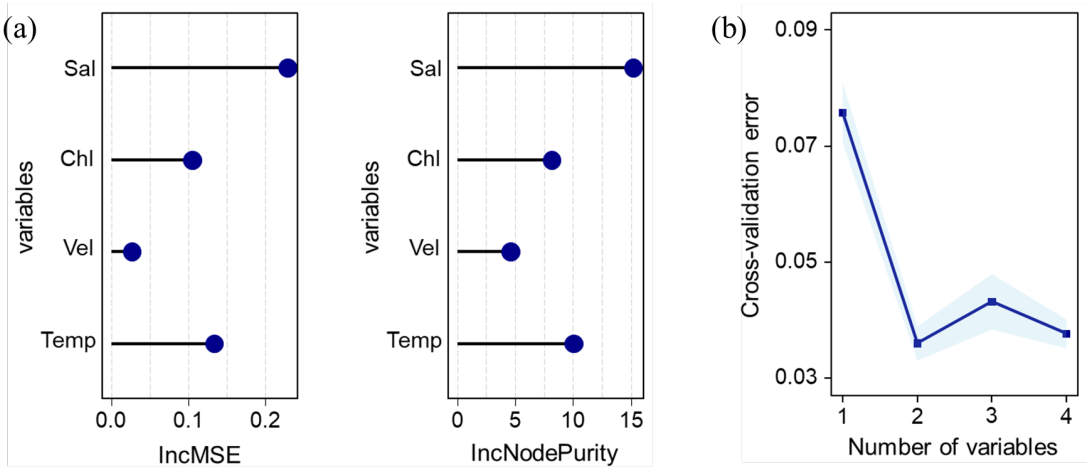

Fig. 2.8 (a) Relative importance of environmental variables (sal = salinity, chl = chlorophyll-a, vel = near-bed velocity, temp = temperature) for flat oyster gaping identified using two evaluation methods, namely increase in mean squared error (InMSE) and increase in node purity (IncNodePurity). (b) Performance of random forest regression models, quantified as error of 10-fold cross-validation results, using different numbers of environmental variables (1 to 4).

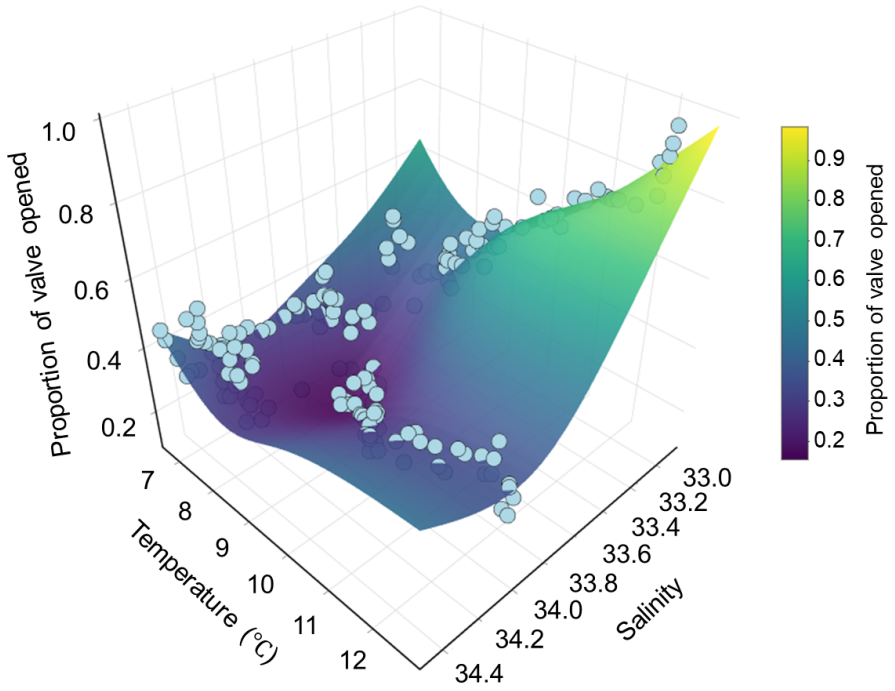

Fig. 2.9 Response of flat oyster gaping (i.e., proportion of valve opened) to key environmental factors including temperature and salinity. The light blue scattered points are real measurement data, and the surface is the fitting result.

2.4 Discussion

Towards research objective-1, we tested the Biophys sensor developed by NIOZ during two years of field campaigns. It can be detected every time flat oysters open for feeding or close due to stress, demonstrating that the Biophys sensor can provide valuable information about flat oyster behavior (including feeding frequency and opening width, and stress responses to environmental changes) under offshore conditions with high frequency. Therefore, this sensor is suitable for assessing whether the target location meets the feeding requirements of flat oysters before commencing restoration activities and for monitoring the long-term health of flat oysters during the restoration process.

Additionally, the data-driven clustering algorithm enabled us to draw some inferences about the gaping activity of flat oysters. Firstly, it can clearly distinguish dates when flat oysters open wider, to a medium extent, or narrower. The identified pattern remained consistent across different monitoring periods, namely the winter of 2021-2022 and the winter of 2022-2023. Secondly, the application of this algorithm can also reveal connections between flat oyster gaping and measured environmental variables. The results suggest that flat oysters tend to open wider on warm days with higher chlorophyll-a and oxygen levels, as well as lower salinity and reduced near-bed orbital velocity. These findings align with previous research on oyster feeding and respiration (Bos et al., 2023b; Tonk et al., 2023). Although this analysis was based on data collected during the winter of 2021-2022, it provides substantial support for our research objective-1. Similar analyses will be applied to the gaping data of flat oysters collected during the winter of 2022-2023, once environmental data becomes available. However, we anticipate similar results, particularly considering the consistent gaping patterns exhibited by flat oysters in the two monitoring campaigns.

Furthermore, the screening of key environmental variables would aid in simplifying habitat suitability assessment procedures while ensuring accuracy. A random forest regression model was applied for this purpose. The results indicated that salinity and temperature are the most crucial factors regulating the gaping behavior of flat oysters in offshore environments. These factors should take precedence when conducting habitat suitability assessments for target restoration sites. Currently, numerous models are available to predict seabed temperature and salinity (e.g., Smith et al., 2007; Tsujino et al., 2020), enabling the assessment of habitat suitability over a broad spatial range and the indirect inference of the long-term health of deployed flat oysters.

Of note, due to technical glitches in the deployed instruments, we relied on open-access environmental data in this study, which left us with limited environmental variables available to explain the observed gaping pattern of flat oysters. Additional environmental variables, such as water turbidity that have the potential to further influence flat oyster gaping, should be simultaneously monitored in situ using relevant instrumentation in future practice. Both of our field campaigns were conducted in winter, during which the variations in environmental parameters were limited and fell within the tolerance range of flat oysters. This, on one hand, confirmed the environmental suitability of the restoration site for flat oyster survival (Bos et al.,

2023a), but on the other hand, it constrains our ability to detect the environmental thresholds that might lead to flat oyster mortality. In future studies, it is recommended to use Biophys sensors to monitor flat oyster gaping in other seasons, particularly in the summer when heatwaves are possible, to gain a more comprehensive understanding of flat oyster feeding and health maintenance.

3. Quantifying critical dislodgement threshold of flat oysters

3.1 Introduction

The flat oyster restoration pilot at the Gemini wind farm aims to kickstart the recovery of a self-sustaining population. The indicator of restoration success is the stability of loosely deployed flat oysters, namely, their ability to remain in place. This depends on the entanglement of the critical dislodgement threshold (i.e., a quantitative parameter of resistance) of flat oysters with instantaneous hydrodynamic disturbances. In this section, we employ an innovative technical approach (i.e., Biophy-logging package) to monitor the dislodgement of loose flat oysters in situ under hydrodynamic forces and thus to achieve our **research objective-2: *Quantifying the critical hydrodynamic conditions (i.e., the critical dislodgement threshold) that result in the dislodgement of loosely deployed flat oysters***. The results are expected to support the assessment and prediction of the long-term stability of restored flat oysters by comparing their critical dislodgement threshold to the evolving hydrodynamic conditions.

3.2 Methods

3.2.1 Biophy-logging package

A retrievable Biophy-logging package was developed in this study to achieve the in-situ monitoring of flat oyster mobility at high-frequency. This package incorporates flat oyster mimics containing accelerometers (MSR-145B4; Fig. 3.1c) and one wave radar (ID: OHVS1), allowing the separate recording of oyster movement acceleration and wave regimes over time. Prior to deployment, accelerometers were carefully placed within empty, fleshless flat oysters and securely affixed using adhesive (Fig. 3.1d). The resulting oyster mimics were comparable in size and weight to adult flat oysters, making it possible to experience the movements of real flat oysters driven by hydrodynamics. A total of 48 oyster mimics containing accelerometers were created.

To deploy them, four metal frames (L×W×H = 3.5×2.5×1.5 m; 50 kg), named Oyster ladders, were custom-made (Fig. 3.1e). The Oyster ladders featured a fishbone-like structure with six branches on both the left and right sides. For each Oyster ladder, 12 oyster mimics containing accelerometers were securely fastened at the trailing end of its 12 branches using high-strength

nylon ropes. This setup ensured that the oyster mimics wouldn't be lost after dislodgement but would, instead, experience increased motion intensity due to hydrodynamic drag. The spacing between the branches of the Oyster ladder was significantly greater than twice the length of the nylon ropes, preventing any interference among the 12 oyster mimics. Each Oyster ladder was equipped with an acoustic release mechanism for retrieval after the monitoring period (Fig. 3.1f).

3.2.2 Field monitoring

The field monitoring was carried out at the Gemini windfarm, situated approximately 85 kilometers off the northern coast of the Netherlands (Fig. 3.1a). In an effort to initiate the recovery of self-sustaining flat oyster reefs, a substantial number of individual flat oysters were loosely deployed in the area. During the winter of 2022-2023, four Oyster ladders, housing a total of 48 oyster mimics equipped with accelerometers, were placed on the seabed at a depth of approximately 32 meters. The layout of Oyster ladders within the Gemini Windfarm is illustrated in Figure 3.1b. The field monitoring commenced on November 13, 2022, and concluded on May 31, 2023, to encompass the occurrence of high-energy hydrodynamic events as much as possible.

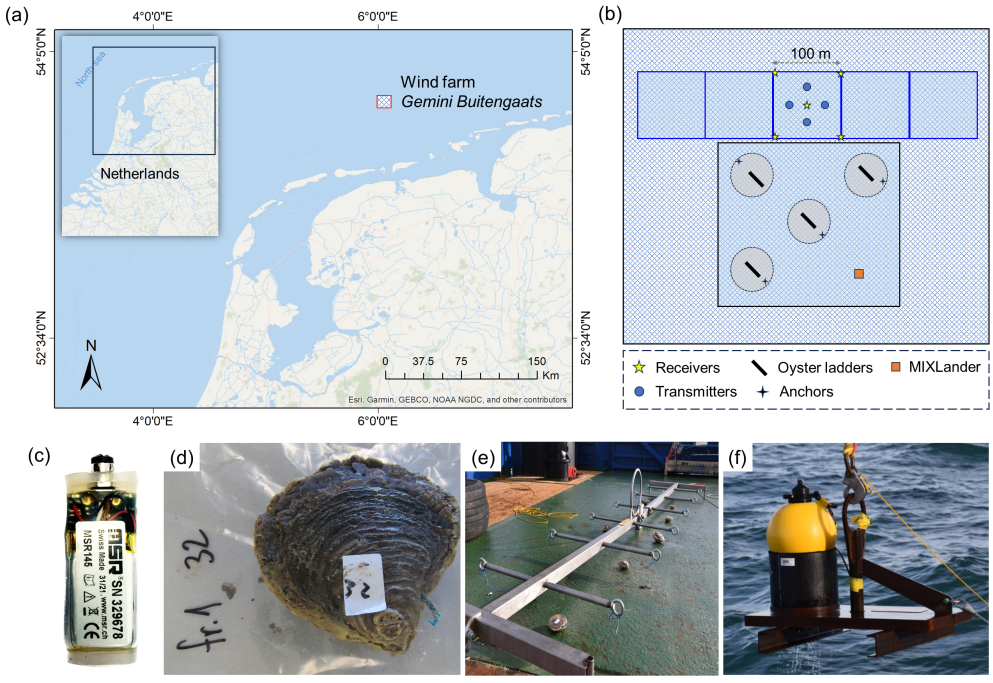

Fig. 3.1 (a) Geographical location of Gemini wind farm. (b) Deployment diagram of Oyster ladders (within the rectangle with black border). The rectangles with blue border represent the restoration

plots, where flat oysters were loosely deployed. The middle plot was used to set up the acoustic telemetry matrix (see Section 4). The orange rectangle indicates the deployment location of MIXLander (see Section 2). (c) Accelerometer used to measure the movement intensity of flat oysters. (d) Photo of the flat oyster mimic, which is a component of the Biophy-logging package. An accelerometer was placed inside the flat oyster after the flesh was removed, and then the shells were sealed using adhesive. (e) The framework (named Oyster ladder) used for deploying flat oyster mimics containing accelerometers on the seabed. The flat oyster mimic is secured to the frame's branch with a rope to prevent loss after dislodgement. (f) Anchor with acoustic release mechanism for securing and retrieving Oyster ladders.

3.2.3 Data analysis

The accelerometers in the Biophy-logging package measure gravitational acceleration (m s^{-2}) in the x, y, and z coordinates at a frequency of 25 s^{-1}. Consequently, they do not measure acceleration induced by currents or individual waves, but rather track changes in orientation at 25-second intervals. These position changes remain negligible when the oyster mimics were stable, but become noticeable when the oyster mimics were in motion, resulting in frequent changes in orientation. The orientation change (δ_{ori}) between each measurement was calculated as follows:

$$\delta_{ori} = \sqrt{{\partial_{a,x}}^2 + {\partial_{a,y}}^2 + {\partial_{a,z}}^2}$$

Where ${\partial_{a,x}}^2$, ${\partial_{a,y}}^2$, and ${\partial_{a,z}}^2$ are the changes in (gravitational) acceleration in the x, y, and z directions, respectively. The measurement frequency of accelerometers is relatively low compared to the wave period. Therefore, δ_{ori} may not fully reflect the movement intensity. For example, multiple orientation changes as waves pass could result in only a small δ_{ori} if the final orientation remains similar, or when mussels are stable except for a single movement during the 25-second measurement interval δ_{ori} may be large. As a result, it is not possible to directly distinguish dislodgement from other movements via δ_{ori} from a single measurement, thus the movement intensity was defined as the sum of δ_{ori} over a 30-minute rolling window.

To interpret the potential movements of deployed oyster mimics, wave data collected by a wave radar (ID: OHVS1) situated at the Gemini windfarm were analyzed (Fig. 3.1a). This wave

radar is located approximately 500 meters from the sites where Oyster ladders were deployed, thus it is considered representative and can be used to explain the movement of oyster mimics. The wave radar measures wave conditions at 15-minute intervals between bursts, with the data presented as significant wave height and corresponding wave period for each 15-minute interval. The movement of oyster mimics is a result of shear stress acting upon them. Estimating the shear stress experienced by the oyster mimics requires evaluating the bed roughness, which would introduce uncertainties. Therefore, we used near-bed orbital velocity as an indicator of the hydrodynamic forces experienced by the oyster mimics instead. The near-bed orbital velocity (u; m s^{-1}) was calculated from water depth and significant wave height via linear wave theory:

$$u = \frac{\omega h_s}{2\sinh[kd]}$$

Where ω is the wave orbital speed (rad s^{-1}), h_s is the significant wave height (m), d is the water depth (m), and k is the wave number, which is calculated as:

$$k = \frac{2\pi}{L}$$

Where L is the wave length (m), which is calculated iteratively from the wave dispersion relation:

$$L = \frac{gT^2}{2\pi}\tanh\left[\frac{2\pi d}{L}\right]$$

Where g is gravitational acceleration (m s^{-2}).

To match the hydrodynamic data, the movement intensity of the oyster mimics was calculated as an average every 15 minutes. Because the Oyster ladders were deployed in close proximity and only one wave radar was available, data from all accelerometers were aggregated to represent the average movement of oyster mimics at the monitoring site. Segmented regression modeling was employed to determine the critical dislodgement threshold, that is the near-bed orbital velocity corresponding to a sudden change in model slope. This was accomplished using threshold regression models with the R package "chngpt". Threshold models were considered only if the Akaike Information Criterion (AIC) was smaller than the corresponding linear and quadratic regression. Therefore, the presented threshold models have superior data fit than the linear or

quadratic regressions. Threshold estimations for the best model type were repeated with 1000 bootstrapped samples to estimate the distribution of each threshold.

3.3 Results

3.3.1 Critical dislodgement threshold of flat oysters

Out of the 48 oyster mimics, 46 were successfully retrieved, while 5 of them contained accelerometers that were not functioning properly. Therefore, a total of 41 functioning accelerometers successfully captured the movement of the deployed oyster mimics during the monitoring period. Overall, no officially named storm events occurred during the monitoring period, but it did encompass both calm and stormy conditions, resulting in multiple dislodgement and recovery cycles (Fig. 3.2a). The most intense movements of oyster mimics occurred in mid-January and early February 2023 (Fig. 3.2b), coinciding with high-energy hydrodynamic events (with peak near-bed orbital velocities reaching up to 0.9 m s^{-1}). According to the results of segmented regression modeling, the deployed oyster mimics remained stable (i.e., they stayed in place) until the near-bed orbital velocity reached 0.45 m s^{-1} (Fig. 3.2c). The interval between 0.45 m s^{-1} and 0.55 m s^{-1} in near-bed orbital velocity was detected as the potential window for sudden changes in oyster status (i.e., stationary vs. in motion; subplot in Fig. 3.2c). Through repeated modeling using near-bed orbital velocities within this range, a value of 0.52 m s^{-1} was identified as the most likely critical threshold (Fig. 3.2c). Once the near-bed orbital velocity exceeded this threshold, the movement intensity of the oyster mimics increased exponentially.

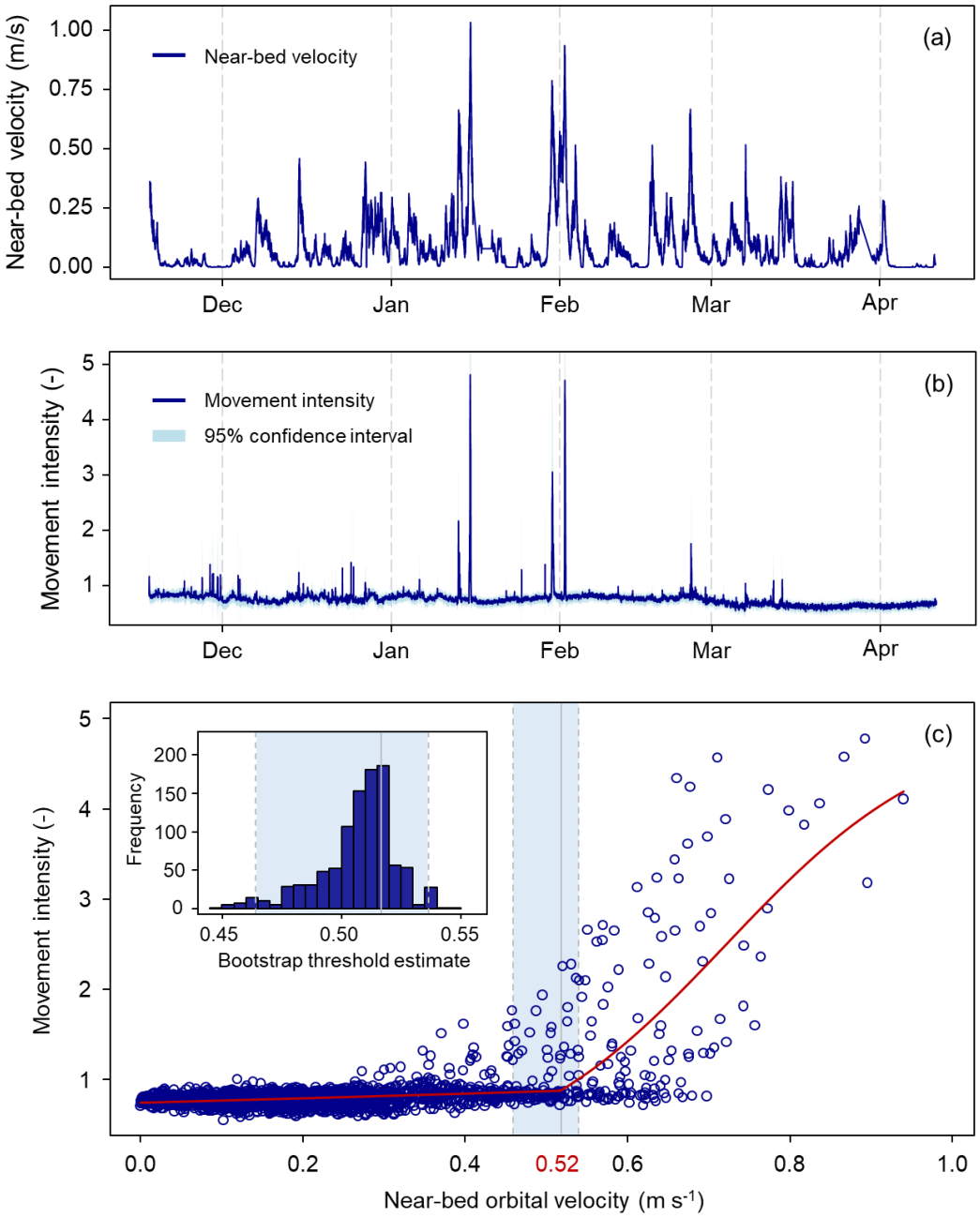

Fig. 3.2 (a) Time-series evolution of hydrodynamic conditions (quantified as near-bed orbital velocity based on significant wave height every 15 minutes) during field monitoring. (b) Movement of oyster mimics recorded by accelerometers during field monitoring. The data is presented as the average movement intensity of 41 oyster mimics recorded by 41 accelerometers with 15-minute intervals. (c) Relationship between oyster movement intensity and near-bed orbital velocity (dark blue scatters) and the segmented regression curves (red line). Segmented regression

was employed to determine the critical dislodgement threshold for oyster mimics, i.e., the near-bed orbital velocity corresponding to a sudden change in model slope. The subplot illustrates the distribution of each potential threshold, which is based on threshold estimations using 1000 bootstrapped samples for the best model type.

3.4 Discussion

Towards research objective-2, we have developed a cost-effective Biophy-logging package, which involves the use of specially designed oyster mimics equipped with accelerometers. This approach allows for the long-term, high-frequency recording of fine-scale movements of flat oysters in response to hydrodynamic disturbances on the seabed, and it enables the correlation of oyster movements with instantaneous hydrodynamic disturbance at a high temporal resolution (in minutes). Here, we used the wave radar deployed in the nearby area and converted the collected wave conditions into near-bed orbital velocities using theoretical formulas. This may introduce some computational errors. For future research and applications, it is recommended to deploy instruments, capable of recording hydrodynamic conditions in-situ over the long term (such as pressure sensor, ADCP or HR with supplementary batteries), alongside the oyster mimics equipped with accelerometers. In this way, the near-bed hydrodynamic disturbances experienced by flat oysters can be reproduced as accurately as possible. Nevertheless, our on-site monitoring has, for the first time, tracked the stability changes of loosely deployed flat oysters during high-energy hydrodynamic periods and quantified the critical hydrodynamic threshold that leads to the dislodgment of these loosely deployed flat oysters.

The hydrodynamic regime at the Gemini wind farm is relatively weak during calm periods, especially before January 2023 and after March 2023. During these times, the flat oyster individuals located on the seabed can maintain a stable state (i.e., remain in place). However, despite no officially named storm events occurring during the monitoring period, a few strong wind events in mid-January to mid-February still caused significant near-bed hydrodynamic disturbances. During these events, the critical dislodgement threshold of flat oysters was exceeded, exposing them to a high risk of drifting and being lost. This risk may significantly increase in years with (multiple) storm events, such as the winter of 2021-2022. Notably, the critical dislodgement threshold (i.e., near-bed orbital velocity = 0.52 m s^{-1}) quantified here for flat oysters supports the

results obtained using acoustic telemetry techniques (see Section-4), where all deployed flat oysters were lost between mid-January and mid-February 2023. In particular, the probability of flat oysters' presence within the acoustic telemetry array was determined to be zero, when the near-bed orbital velocity exceeded 0.52 m s^{-1} (Fig. 4.7).

Overall, the evolution of hydrodynamic regimes, especially during the winter season, should be recognized as the primary habitat suitability assessment parameter for the restoration practices dedicated to the loose deployment of flat oysters. Connecting this parameter with the critical dislodgment threshold of flat oysters enables the assessment of the stability of restored materials over time. The Biophy-logging package we have developed can efficiently provide information for this purpose. Additionally, this monitoring approach holds the potential for broader applications in other comparable underwater ecosystems to assess the mobility of organisms.

4. Tracking the movements of loosely deployed flat oysters

4.1 Introduction

Once the target location is identified as suitable for sustaining the healthy growth of flat oysters, the implementation of the restoration pilot is possible. In the Gemini wind farm, this involves the loose deployment of flat oysters. A crucial question emerges: what happens to the flat oysters after being loosely deployed at the target location? Especially during storm seasons, are they at risk of being washed away? In essence, a widely dispersed oyster population cannot serve as the starting point/incubator for a reef (Bos et al., 2023b). Understanding the fate of flat oysters hinges on effective tools to decipher where, when, and how they move. Notably, movement is a fractal process; hence, the scale (spatial and temporal) of observation significantly influences the results (Lennox et al., 2023). The most common approach is to regularly visit the restoration location and use remotely operated vehicles (ROVs) to survey the presence of flat oysters (van Der Reijden et al., 2019; Esagholian et al., 2021). However, this method can only qualitatively inform whether the flat oysters remain at the restoration location at specific points in time, without providing insights into the continuous time series of flat oyster activity patterns (Esagholian et al., 2021). In this section, we employ an innovative method of acoustic telemetry to achieve precise location calculations for the loosely deployed flat oysters, enabling the ***tracking of their long-term activity trajectories and ranges*** (i.e., our research **objective-3**). By integrating data regarding oyster characteristics and from the surrounding environment, we expect to uncover the key factors driving the fate of flat oysters after their loose deployment.

4.2 Methods

4.2.1 Acoustic telemetry

Acoustic telemetry refers to the use of sound (acoustics) to relay information across open space (telemetry). An acoustic telemetry system consists of two main components:

- *Transmitter*: an electronic tag that broadcasts a series of “pings” (sound pulses) into the surrounding water. Details of the transmitters used in this study are available at https://www.thelmabiotel.com/transmitters/6mm/.

- *Receiver*: A compact data-logging computer that "listens" for pings from transmitters. Upon signal detection, the transmitter's unique ID code, along with the time and date, is recorded. Details of the receiver used in this study are available at https://www.thelmabiotel.com/receivers/mooring-recovery-system/.

In our application, transmitters were affixed to the shells of loosely deployed flat oysters (Fig. 4.1). A telemetry array consisting of five receivers was deployed at the restoration to "listen" for the distinctive sound pulses emitted by the transmitters on each flat oyster. These receivers have known precise coordinates and are configured with synchronized clocks with millisecond precision. Similar to GPS technology, the telemetry array uses the difference in time it takes for a signal to be "heard" by three or more receivers to "triangulate" the position of a flat oyster (Lennox et al., 2023).

4.2.2 Field monitoring

In the winter of 2022, over 1,500 flat oysters and 18 tons of shell material were deployed at the Gemini wind farm (Fig. 4.1a), approximately 85 kilometers off the northern coast of the Netherlands, to initiate the restoration of a self-sustaining flat oyster reef. Our field monitoring coincided with this restoration activity at the same location.

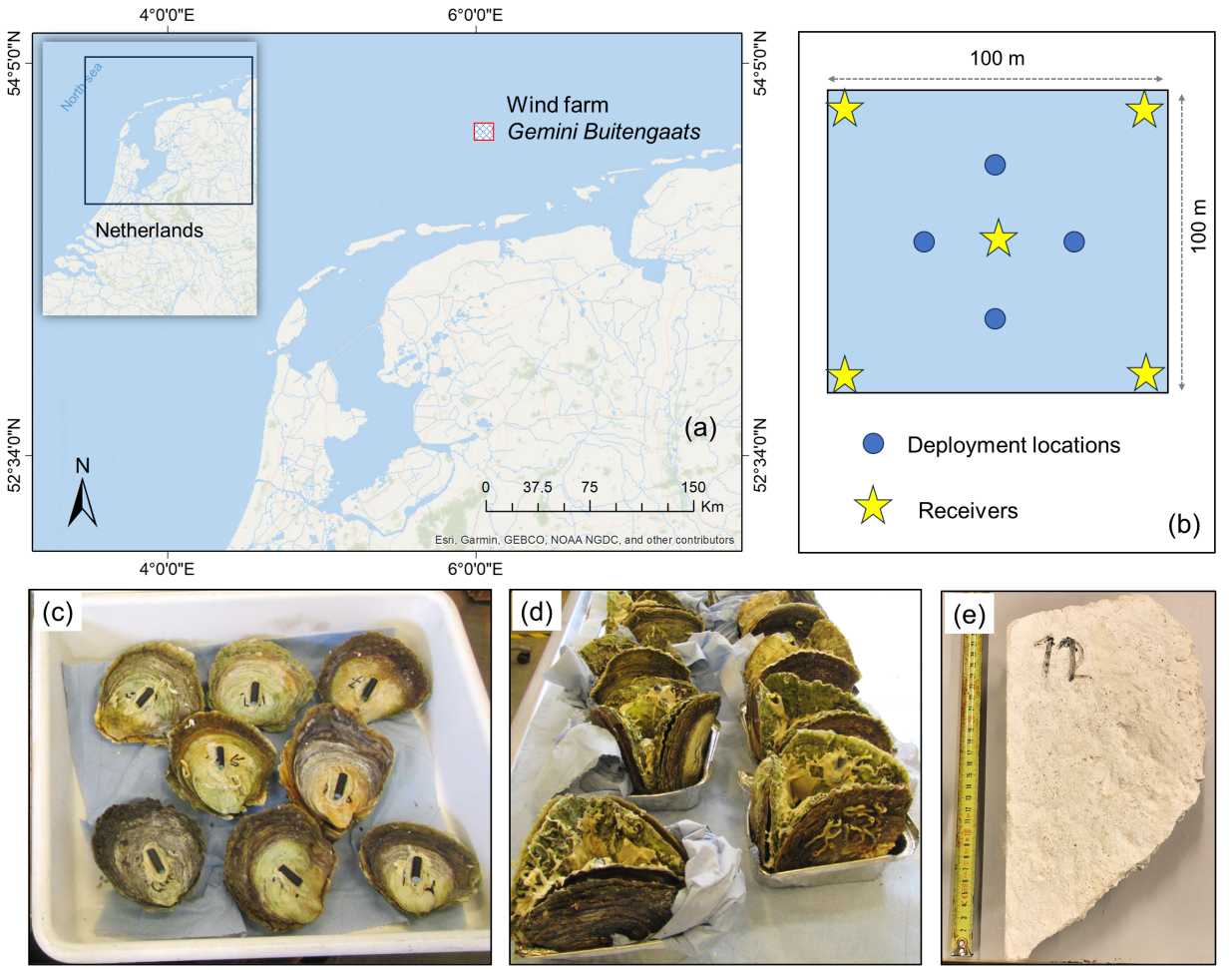

Fig. 4.1 (a) Geographic location of the Gemini wind farm. (b) Schematic layout of the acoustic telemetry array consisting of five receivers. Monitoring units, which included flat oyster individuals (c), clusters (d), and BESE chunks (e), were lowered into the deployment locations along with shell material. Each monitoring unit was attached with an acoustic tag to enable the monitoring of their movement trajectory and range.

A total of 121 wild flat oysters sourced from Norway were pre-collected for tracking the activities of loosely deployed flat oysters during field monitoring. 66 of these flat oysters were assembled into oyster clusters, each comprising three individuals fixed together with adhesive, to mimic larger oyster groups that may exist in reality (thus representing greater mass). This resulted in 55 individual flat oysters and 22 flat oyster clusters, each of which was attached with an acoustic tag (i.e., the transmitter; Fig. 4.1c, d). Additionally, the BESE chunks (Fig. 4.1e) are considered as

the most promising degradable substrate for flat oyster settlement. As an exploratory initiative, we prepared 11 BESE chunks, each equipped with an acoustic tag, to monitor and assess their stability.

During the on-site deployment, shell material was first packed into four big bags. Flat oyster individuals, clusters, and BESE chunks with attached acoustic tags were divided into four sets. Each set, along with flat oysters used for restoration, was placed above the shell material in each big bag (Fig. 4.2a). Subsequently, these four big bags were lowered into the seabed at four separate locations within a one-hectare area, allowing the shell material, along with flat oysters, to drop from the openings at the bottom of the bags (Fig. 4.2b, c). To detect the signals of acoustic tags, five receivers were mounted on custom frames (L×W×H = 2.5×2.5×3 m; 1500 kg; Fig. 4.2d), and then deployed at the corners and center of this one-hectare area, forming an acoustic telemetry array (Fig. 4.1b). If any movement occurred from flat oyster individuals, clusters, or BESE chunks within this array, the receivers would record the signals from the corresponding acoustic tags. Each receiver was equipped with an acoustic release mechanism (Fig. 4.2d) to facilitate retrieval after the monitoring period.

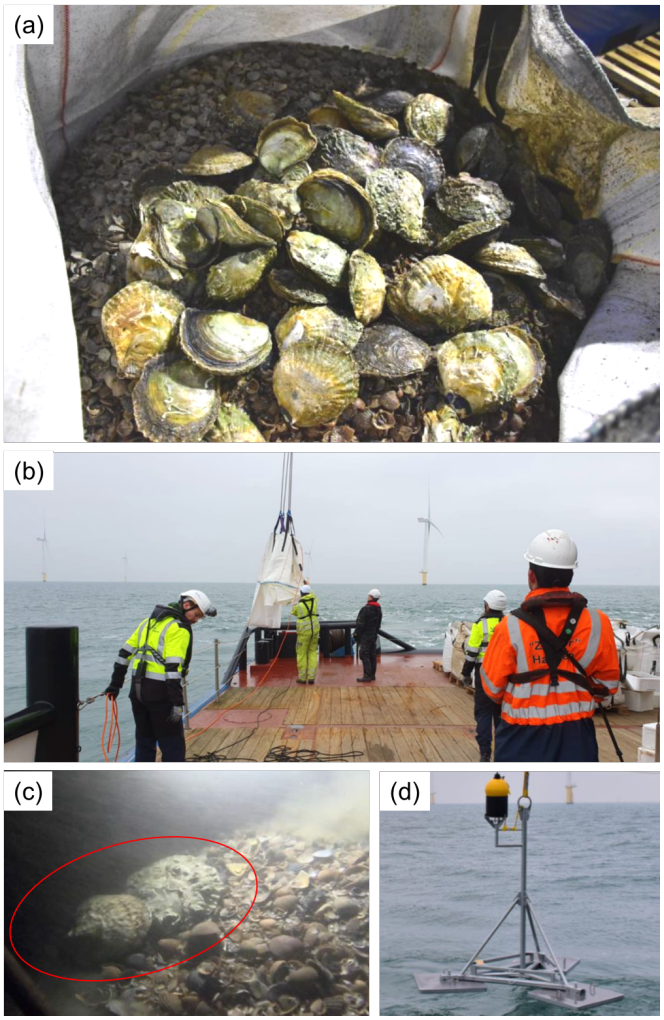

Fig. 4.2 (a) Flat oyster individuals and clusters with acoustic tags, along with flat oysters used for restoration, were placed inside large bags filled with shell material. (b) The large bag was lowered to the seabed, allowing all contents to drop from the openings at the bottom. (c) A drop-cam showed the shell material with loosely deployed flat oysters on the seabed. (d) The custom-made frame for deploying the receiver, which is also equipped with an acoustic recovery device.

In April 2023, a total of 62 flat oyster mimics with attached acoustic tags were supplementary deployed within the acoustic telemetry array. Unlike the previous deployment, these flat oysters were deactivated and sterilized to avoid the introduction of diseases. Adhesive was used to fill the shells to replicate the weight of live flat oysters and to seal the shells. All

receivers were retrieved at the end of May 2023, and the collected data were downloaded for subsequent analysis.

4.2.3 Environmental datasets

Temperature, near-bed orbital velocity, and bed-level change were considered as potential environmental variables influencing the movement of flat oysters. Details on the collection and processing of temperature and near-bed orbital velocity dataset were described in Section 2.2.3. The bed-level change was measured using ASED sensors developed by NIOZ. These sensors were installed on the MIXLander (see Section 2.2.3), which were deployed approximately 220 m away from the study area. The ASED sensor measured its distance to the seafloor at an interval of 30 min. The initial height was set as a reference, and the subsequent measurements were subtracted from it to characterize the bed-level changes (positive values indicating accretion, and negative values indicating erosion). Data from the four sensors were combined, and daily (or weekly) averages were calculated to obtain manageable time series data for subsequent analysis.

4.2.4 Data processing and analysis

Raw detections were pre-processed by Thelma Biotel (https://www.thelmabiotel.com/) to determine pinpoint high spatial resolution positions. A brief overview of the algorithm process follows below:

1) Import tag data with synchronized receiver clocks.
2) Estimate signal propagation speed.
3) For each transmit detected on at least 3 receivers:
    a) Geometry checks to avoid receiver constellations with high probability for poor position fixes. If accepted, the algorithm creates a table of equations based on time difference of arrival.
    b) Pinpoint uses information from all receivers detecting the same transmit to minimize the least square error. The solver (Levenberg-Marquardt's method) also includes information about receiver and transmitter depth. When several triangles locate the same transmitter,

Pinpoint calculates a weighted average, prioritizing the triangles with lowest HDOP (horizontal dilution of precision).

c) If the solution is found inside an area with acceptable error sensitivity, it is accepted.

The final output consists of pinpoint positions for each transmitter throughout the time series. These positions are subsequently used to ascertain the behavioral features of each corresponding deployed unit (i.e., flat oyster individual, cluster, or BESE chunk), including residency, movement speed, and activity space.

Pairwise correlation analysis was used to detect potential associations between environmental variables and their associations with time (i.e., days after deployment or weeks after deployment). Variables with a correlation coefficient $|\rho| > 0.6$ were considered autocorrelated. It was found that only near-bed orbital velocity had no significant correlation with time (Fig. 4.3). This may be attributed to the short residence period (less than three months; see section 4.3.1) of deployed units, which does not allow for high variability in temperature and bed level. As a result, only the near-bed orbital velocity can be used for subsequent correlation with the movement of deployment units.

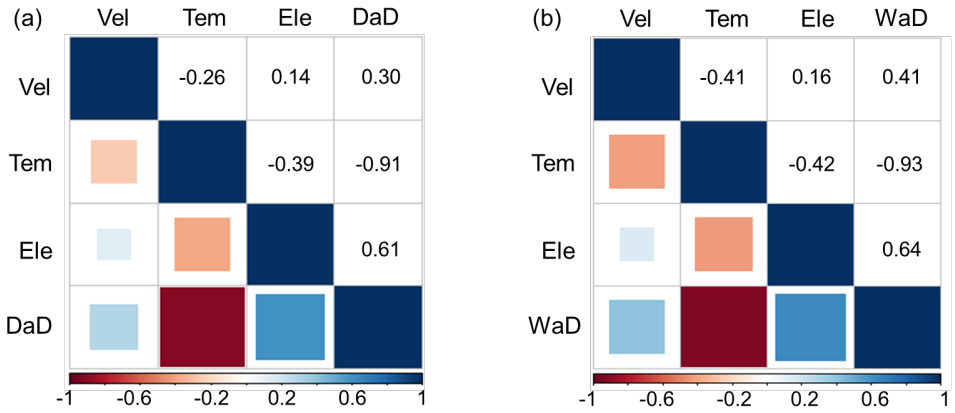

Fig. 4.3 Results of pairwise correlation analysis regarding daily average (a) and weekly average (b) of environmental variables. Vel: Near-bed orbital velocity; Tem: Temperature; Ele: relative bed-level change; DaD: Days after deployment; WaD: Weeks after deployment.

4.2.3.1 Residency

To quantify the overall residency of deployed units (including flat oyster individuals, clusters and BESE chunks, hereafter simplified as units) in the study area, a residency index (RI; Espinoza et al., 2011) was calculated for each unit based on the number of days the transmitter was detected.

$$RI = \frac{\mathrm{DD}}{\mathrm{TD}}$$

where (DD) is the number of days the unit was detected, and (TD) is the number of days between deployment date and the end of the study. The (RI) ranges from 0 (indicating no residency) to 1 (indicating absolute residency within the study area).

To elucidate the driving factors behind residency variation among units, the probability of being present in the study area on any given date was calculated: 1 = present, 0 = absent (binomial distribution). Subsequently, a Generalized Additive Mixed Effects Model (GAMM) was employed to elucidate the relationship between the residency and explanatory variables.

$$P_{it} = \alpha + \beta_1 Type_i + s(Weight_i) + s(Velocity_t) + a_i + \varepsilon_{it}$$

where P_{it} is the present probability of unit i on day t in the study area. Parameter explanatory variable is $Type_i$ (a categorical variable with three levels – individual, cluster and BESE) with its linear coefficient β_1. $Weight_i$ (weight of deployment units) and $Velocity_t$ (daily averaged near-bed orbital velocity) were fitted as non-parametric smoothing functions s.

4.2.3.2 Movement speed

The following analysis is limited to flat oyster individuals and clusters, given the small sample size of BESE chunks (Table 4.1) and their lack of autonomous movement capability.

Trajectories for each oyster individual and cluster were computed based on consecutive pinpoint positions. Individual trajectories were segmented into sub-trajectories to exclude cases where two consecutive unit' positions were separated by more than 24 hours, assuming no movement occurred in such instances. Sub-trajectories composed of fewer than four positions were

excluded. Finally, interpolation was applied to each sub-trajectory at intervals of 600 seconds to obtain regular sub-trajectories for speed computation (Papadopoulo et al., 2023). The choice of a 600-second time interval was made to align with the minimum possible delay of the transmitters. Therefore, segmenting the time series into 600-second intervals allowed for interpolation without losing any original positions. Speed (in meters per second) was calculated as a proxy for activity (Zamora & Moreno, 2002) as:

$$Speed = \frac{dist}{dt}$$

where $dist$ is the distance travelled between each pair of consecutive positions in the interpolated sub-trajectories and dt equals 600 s.

GAMM with following structure was employed to elucidate the nonlinear relationship between the speed and explanatory variables:

$$Speed_{it} = \alpha + \beta_1 Type_i + s(Weight_i) + s(Velocity_t) + a_i + \varepsilon_{it}$$

where $Speed_{it}$ is the averaged movement speed of unit i on day t. Parameter explanatory variable is $Type_i$ (a categorical variable with two levels – individual and cluster) with its linear coefficient β_1. $Weight_i$ (weight of flat oyster individuals or clusters) and $Velocity_t$ (daily averaged near-bed orbital velocity) were fitted as non-parametric smoothing functions s.

4.2.3.3 Activity space

The following analysis is limited to flat oyster individuals and clusters, given the small sample size of BESE chunks (Table 4.1) and their lack of autonomous movement capability.

To investigate the activity space of flat oyster individuals and clusters within the study area, the 95% Kernel Utilization Distribution (KUD; Hays et al., 2021) for each unit was computed using the positions of transmitters. KUD were calculated for each week and for the entire study period using the entire dataset. To mitigate potential biases in activity space calculations, weeks with less than 4 days of detection were excluded from KUD calculations, regardless of whether these days were consecutive (Papadopoulo et al., 2023).

GAMM with following structure was employed to elucidate the nonlinear relationship between the activity space and explanatory variables:

$$AS_{it} = \alpha + \beta_1 Type_i + s(Weight_i) + s(Velocity_t) + a_i + \varepsilon_{it}$$

where AS_{it} represents the activity space within the study area of unit i in week t. Parameter explanatory variable is $Type_i$ (a categorical variable with two levels – individual and cluster) with its linear coefficient β_1. $Weight_i$ (weight of flat oyster individuals or clusters) and $Velocity_t$ (weekly averaged near-bed orbital velocity) were fitted as non-parametric smoothing functions s.

Data processing and analysis were conducted using R version 4.2.2. Spatial data were handled using the "leaflet" and "sf" package. The "adehabitatLT" and "ctmm" packages were employed in R for calculating trajectories and KUD for each individual, respectively. All GAMM models were fitted using the "mgcv" package.

4.3 Results

4.3.1 Residency

For the winter deployment campaign conducted in 2022, 49 out of 55 tagged flat oyster individuals, 21 out of 22 tagged flat oyster clusters, and 9 out of 11 tagged BESE chunks were detected in the acoustic telemetry array during the study period (Table 4.1). 12 of the detected flat oyster individuals either disappeared shortly after being tagged (left the array; i.e., transmitter ID = 5346, 5334, 5328, 5301, 5292, 5274, 5271, 5241, 5184, 5178, 5145; Fig. 4.4) or appeared only in the later stages (initially absent; i.e., transmitter ID = 5295; Fig. 4.4). These individuals were deemed non-representative and were subsequently excluded from subsequent analysis. The remaining flat oyster individuals exhibited significant variations in their residency patterns, with an average residence index (RI) of 0.30 (range 0.18–0.42). Among the detected flat oyster clusters, 5 were excluded from analysis for being considered non-representative, because they were either disappeared shortly after being tagged (left the array; i.e., transmitter ID = 5190, 5166, 5163; Fig. 4.4) or appeared only in the later stages (initially absent; i.e., transmitter ID = 5250, 5142; Fig. 4.4). The remaining clusters had an average RI of 0.31 (range 0.22–0.41). Regarding BESE chunks, 3 were excluded because they were disappeared shortly after being tagged (left the array; i.e.,

transmitter ID = 5406, 5400, 5373; Fig. 4.4), and the remaining BESE chunks had an average RI of 0.27 (range 0.22–0.33). The low RI values indicated that the deployed oyster individuals, clusters, and BESE chunks remained within the study area for a shorter period of time. During residency, short disappearances and reappearances of flat oyster individuals and clusters were observed (Fig. 4.4). Reasons for this phenomenon may include: (1) They may temporarily left the range of the acoustic telemetry array but subsequently returned, either due to autonomous movement or the influence of hydrodynamic forces; (2) They may be temporarily buried by sediments, rendering the transmitter signal undetectable. (3) The positioning quality control program excluded the corresponding data when the signal was detected by less than three receivers (see Section 4.2.4).

Table 4.1 Statistics on the number of monitoring units (including oyster individuals, clusters, and BESE chunks) involved in field deployment, signal detection and subsequent analysis.

Units	Deployed	Detected	Analyzed
2022 winter field campaign			
Oyster individuals	55	49	37
Oyster cluster	22	21	16
BESE chunks	11	9	6
2023 spring field campaign			
Oyster mimics	62	9	0
In total	150	88	59

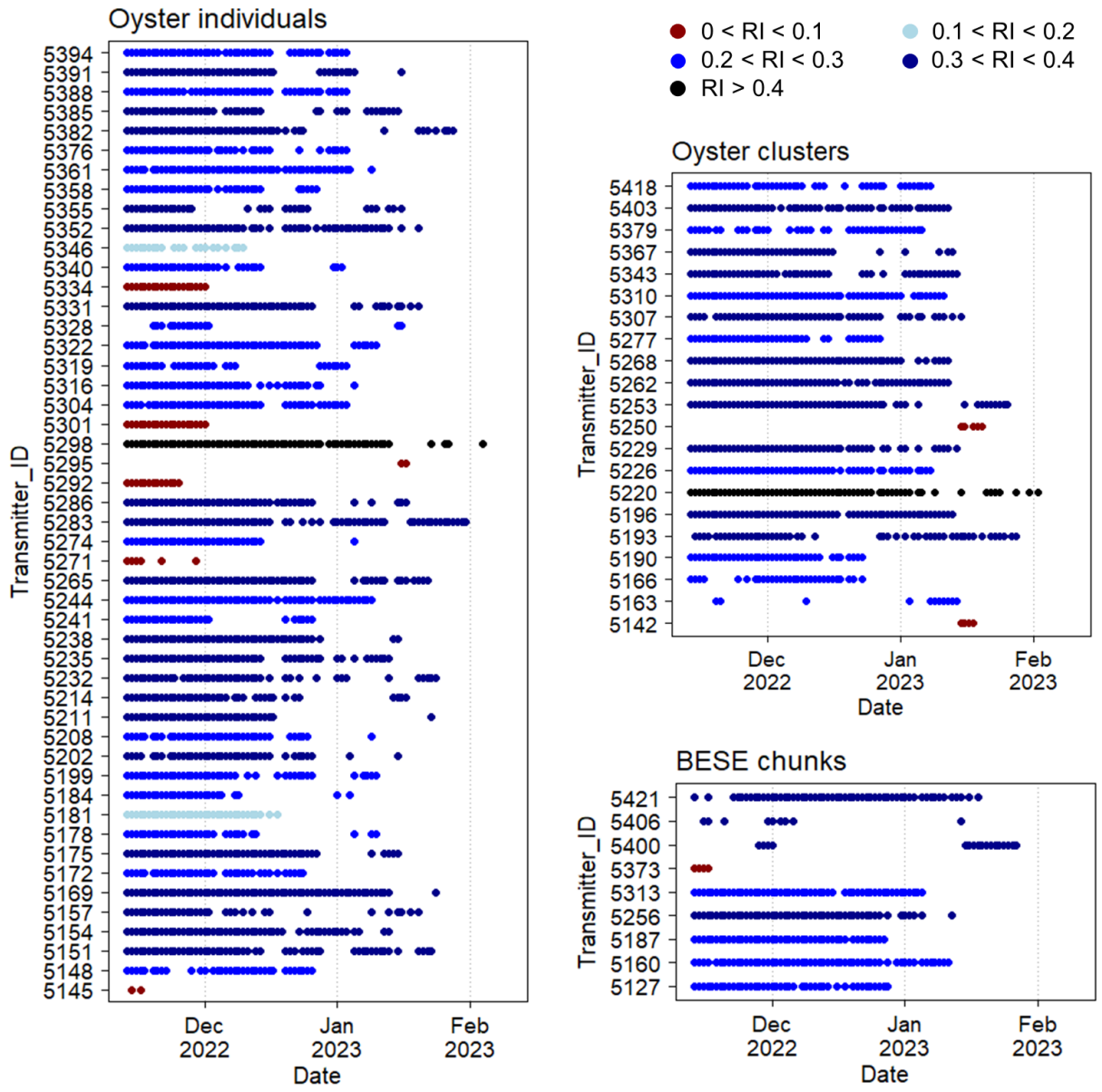

Fig. 4.4 Abacus plot showing the daily presence of monitoring units (including oyster individuals, clusters, and BESE chunks) in the acoustic telemetry array. Plot color depends on the residence index (RI) of the monitoring unit over the entire monitoring period (November 13, 2022 to May 31, 2023). The timeline is cropped to increase detail readability. After the corresponding date, the signals of all monitoring units were no longer detected.

Results regarding the probability of presence provide evidence for our assertion: the deployed oyster individuals, clusters, and BESE chunks remained within the study area for a shorter period of time (Fig. 4.5). During the initial monitoring phase, all units (including oyster individuals, clusters, and BESE chunks) were consistently present (with a probability close to 1). As time progressed, an increasing number of units departed from the array, with a notable decrease in presence occurring from January to February (Fig. 4.5). The latest recorded departure date for the last oyster individual from the array was February 4, 2023. For oyster clusters, the latest departure date was February 2, 2023, and for BESE units, it was January 18, 2023. No signals were detected by the receivers after these respective dates (Fig. 4.5), suggesting that none of units returned to the array after leaving. Upon visualizing the pinpoint positions, it was observed that the units gradually approached the edges of the array from late January to early February (Fig. 4.6). This further confirmed that the deployed oyster individuals, clusters, and BESE chunks left the study area.

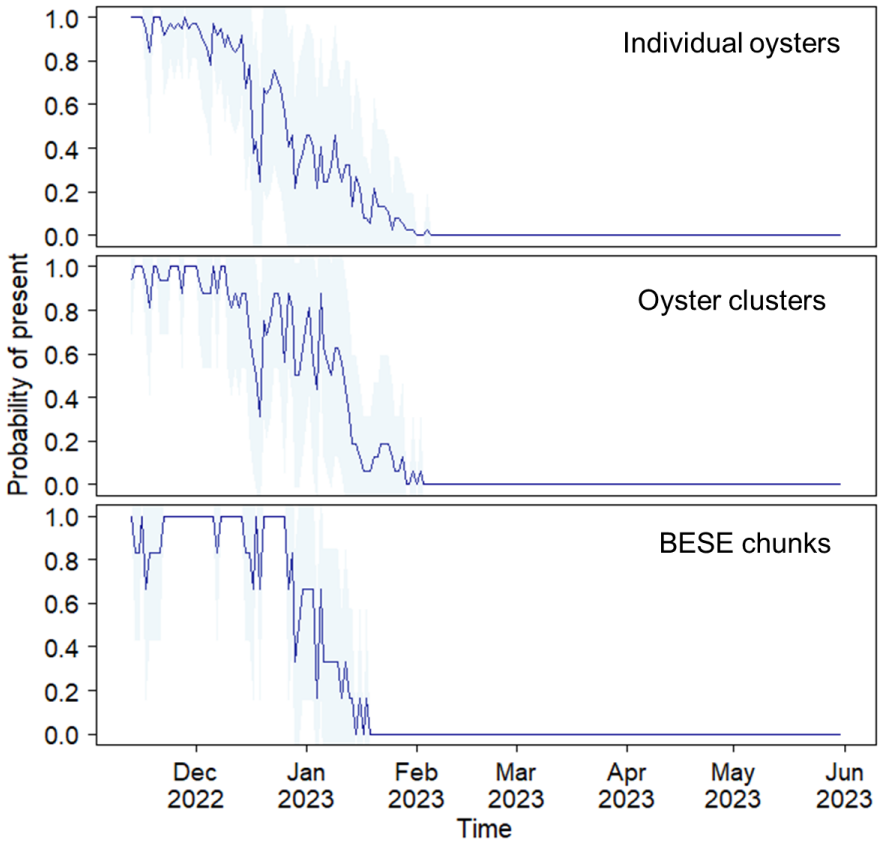

Fig. 4.5 Probability of monitoring units (including oyster individuals, clusters, and BESE chunks) being present in the acoustic telemetry array over time. The dark blue solid line represents the daily

average present probability of the corresponding monitoring unit, and the light blue background represents the 95% confidence interval.

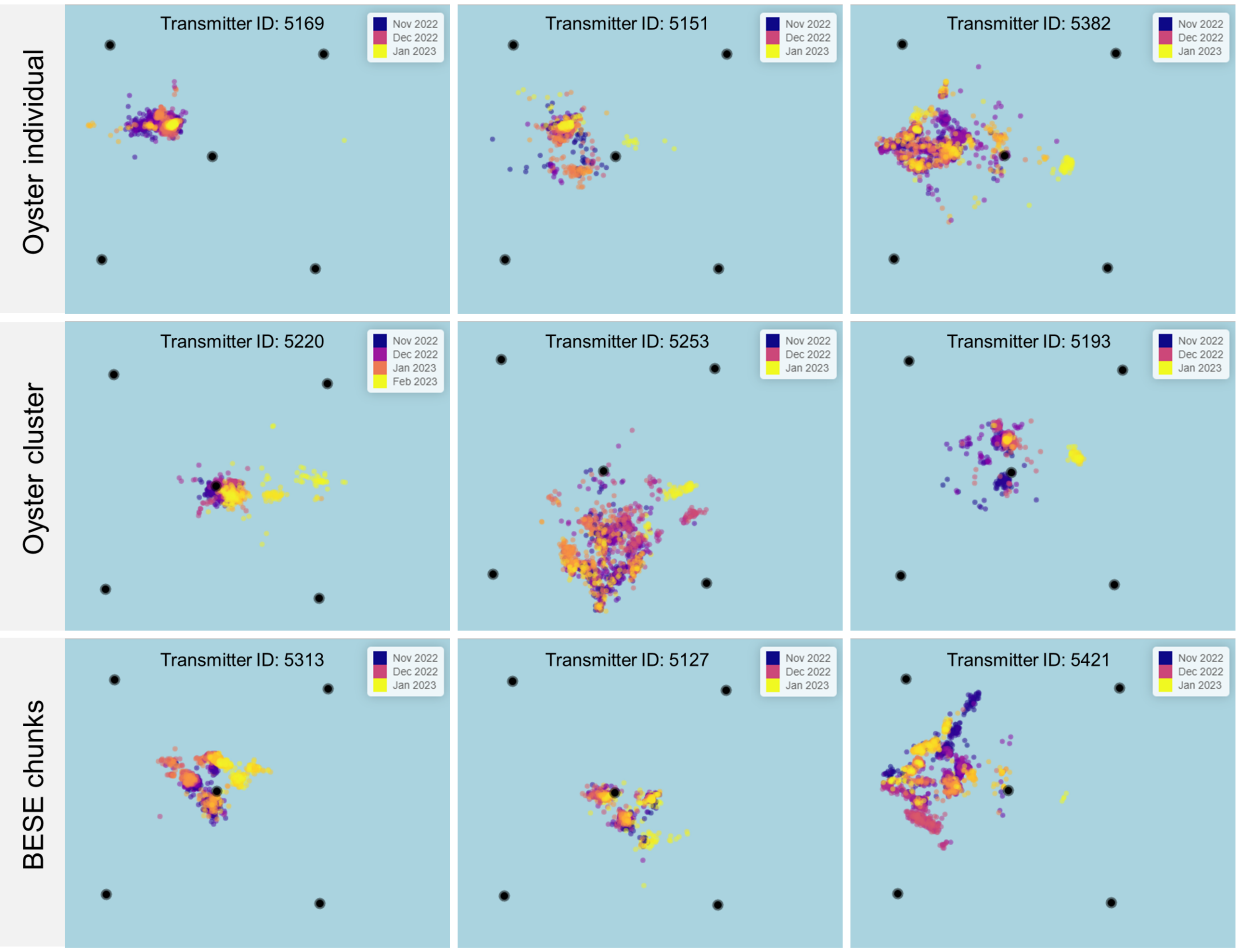

Fig. 4.6 Examples of pinpoint positions of monitoring units, including flat oyster individuals, clusters, and BESE chunks. The black dots represent the distribution of an acoustic telemetry array consisting of five receivers. The color of scatter points indicates temporal changes in pinpoint positions: blue indicates the early stage of monitoring, and yellow indicates the late stage of monitoring. It is evident that during the late stages, all units tended to move toward the edge of the array, suggesting that they likely subsequently left the array.

GAMM results showed that the probability of presence within the study area did not differ significantly between types of units (i.e., flat oyster individual and cluster) and was not significantly affected by their weight (Table 4.2; Fig. 4.7b, c). Near-bed orbital velocity was found to influence the probability of presence within the study area in nonlinear ways (Fig. 4.7a). As the near-bed orbital velocity increased, there was an overall decreasing trend in the probability of presence (Fig. 4.7a). It is worth noting that when the near-bed orbital velocity exceeded 0.52 m s^{-1}, the probability of presence tended to 0 (Fig. 4.7a), which is consistent with the critical dislodgement threshold of flat oysters that we quantified in Section-3 (Fig. 3.2).

Table 4.2 Summary of the Generalized Additive Mixed Effects Model (GAMM) investigating the nonlinear relationship between different behavioral features (probability of presence, movement speed and activity space) of monitored units and explanatory variables.

Parametric coefficients	Estimates	Std error	*t*-Value	Pr(>|t|)
Probability of presence				
Intercept	0.587	0.083	7.049	< 0.001***
Type	-0.091	0.118	-0.776	0.438
Smooth terms	*Edf*	*Ref.df*	*F*	*P-value*
s(weight)	1.489	1.489	0.362	0.726
s(velocity)	8.117	8.117	72.757	< 0.001***
Movement speed				
Intercept	0.003	0.001	2.685	0.007
Type	-0.001	0.002	-0.322	0.747
Smooth terms	*Edf*	*Ref.df*	*F*	*P-value*
s(weight)	2.124	2.124	1.66	0.194
s(velocity)	5.757	5.757	57.02	< 0.001***
Activity space				
Intercept	488.1	315.7	1.546	0.123
Type	330.4	453.1	0.729	0.466
Smooth terms	*Edf*	*Ref.df*	*F*	*P-value*
s(weight)	2.098	2.098	3.466	0.041*
s(velocity)	3.358	3.358	1.679	0.189

Note: Std error: Standard error; Edf: effective degrees of freedom; Ref.df: reference degrees of freedom; R-sq.(adj): adjusted coefficient of determination; Type: type of monitored units; Weight; weight of monitored units; Velocity, near-bed orbital velocity (m s^{-1}). Significance codes: *** 0; ** 0.001; * 0.01.

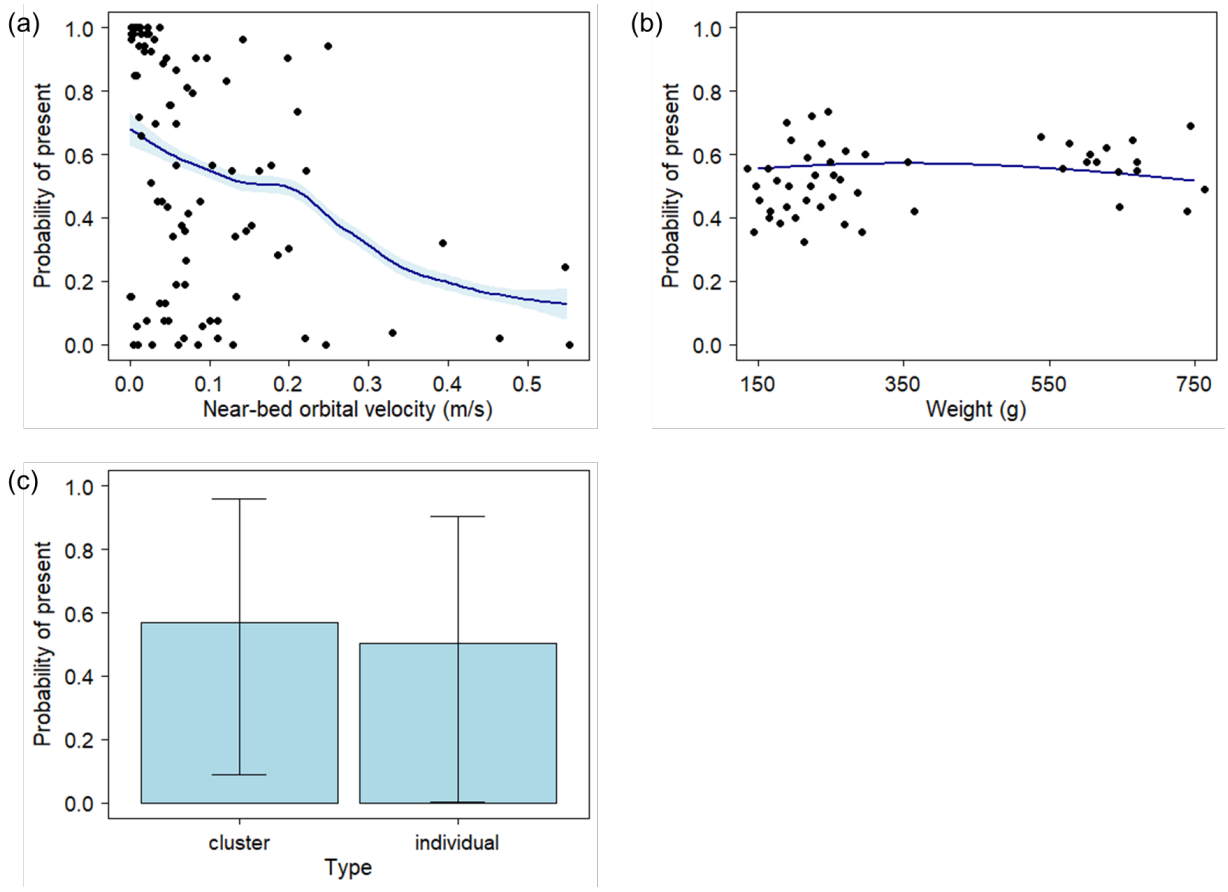

Fig. 4.7 Probability of presence of flat oyster individuals and clusters in the study area as a function of near-bed velocity (a), weight (b) and type (c). In subplot a and b: the black scattered points (a, b) are the statistical results of the measured data (i.e., the average probability at each velocity or weight); the dark blue curve is the fitting result of the GAMM (Generalized Additive Mixed Effects Model); the light blue shaded area represents the 95% confidence interval. Note that the probability of present approaches 0 when the near-bed orbital velocity exceeds 0.52 m s^{-1} (a), which consistent with the critical dislodgement threshold identified in Section 3 (see Fig. 3.2).

For the spring deployment campaign in 2023, only 9 out of the 62 tagged flat oyster mimics were detected in the acoustic telemetry array during the study period (approximately 2 months; Table 4.1). Furthermore, only one mimic was continuously detected throughout and remained within the study area at the conclusion of the monitoring (Fig. 4.8). The loss of signal may be attributed to imprecise positioning during deployment, causing the oyster mimics to be placed

outside the acoustic telemetry array. Consequently, subsequent analysis of the movement of this batch of flat oysters (mimics) was rendered unfeasible.

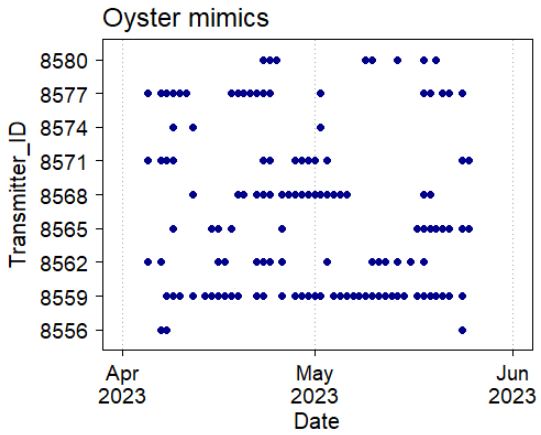

Fig. 4.8 Abacus plot showing the daily presence of monitoring units (i.e., oyster mimics) in the acoustic telemetry array during the monitoring period (April 4, 2023 to May 31, 2023).

4.3.2 Movement speed of flat oysters

Based on the pinpoint positions, the movement trajectories of flat oyster individuals and clusters within the acoustic telemetry array were plotted (Fig. 4.9), allowing the calculation of their movement speeds before leaving the array. These movement was presumed to be autonomous activity of oysters during their residency, as these movements occurred under calm hydrodynamic environments where the near-bed orbital velocity is far below the critical dislodgement threshold (see Section-3) of flat oysters. Overall, the movement speed of flat oyster individuals during their residency ranged from 0 to 0.09 m s^{-1}, with an average of 0.003 m s^{-1}. For flat oyster clusters, their movement speed during residency ranged from 0 to 0.08 m s^{-1}, with an average of 0.003 m s^{-1}.

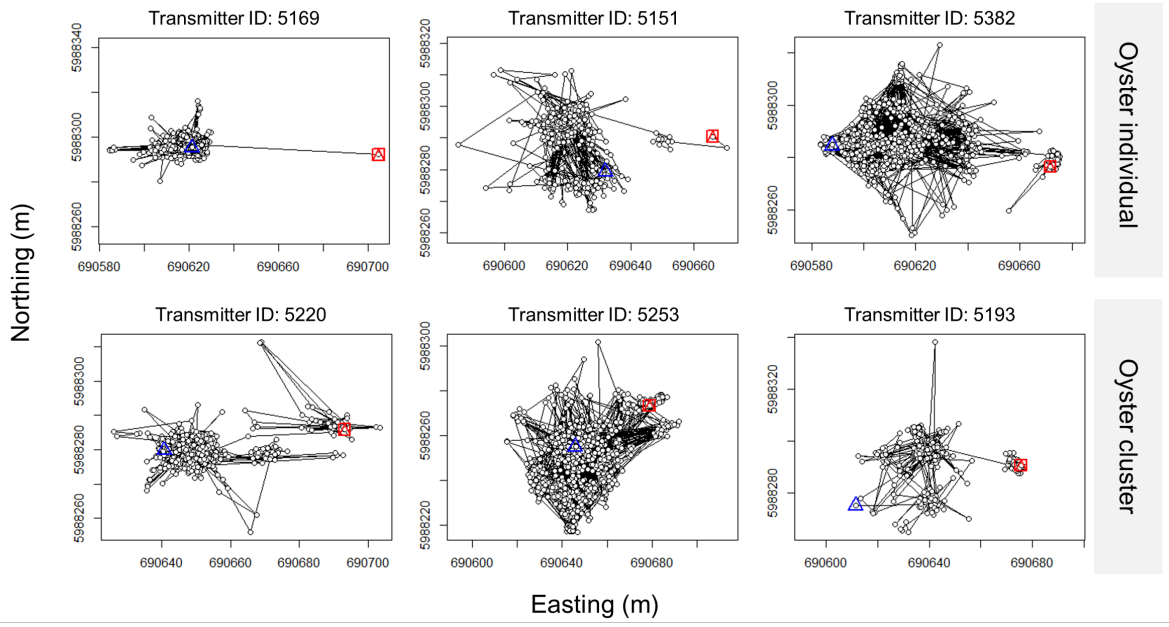

Fig. 4.9 Examples of the movement trajectories of flat oyster individuals and clusters during their residency. Blue triangles represent the initial positions, while red squares indicate the last detected positions. The trajectories were used to determine the distance between paired pinpoint positions, thereby enabling the calculation of the movement speed of flat oyster individuals and clusters.

GAMM results showed that movement speed was not significantly related to type (i.e., flat oyster individual and cluster) and weight, but was regulated by near-bed orbital velocity (Table 4.2; Fig. 4.10b, c). Interestingly, faster movement speeds occurred under conditions of lower near-bed orbital velocity, while slower movement speeds were observed under conditions of higher near-bed velocity (Fig. 4.10a).

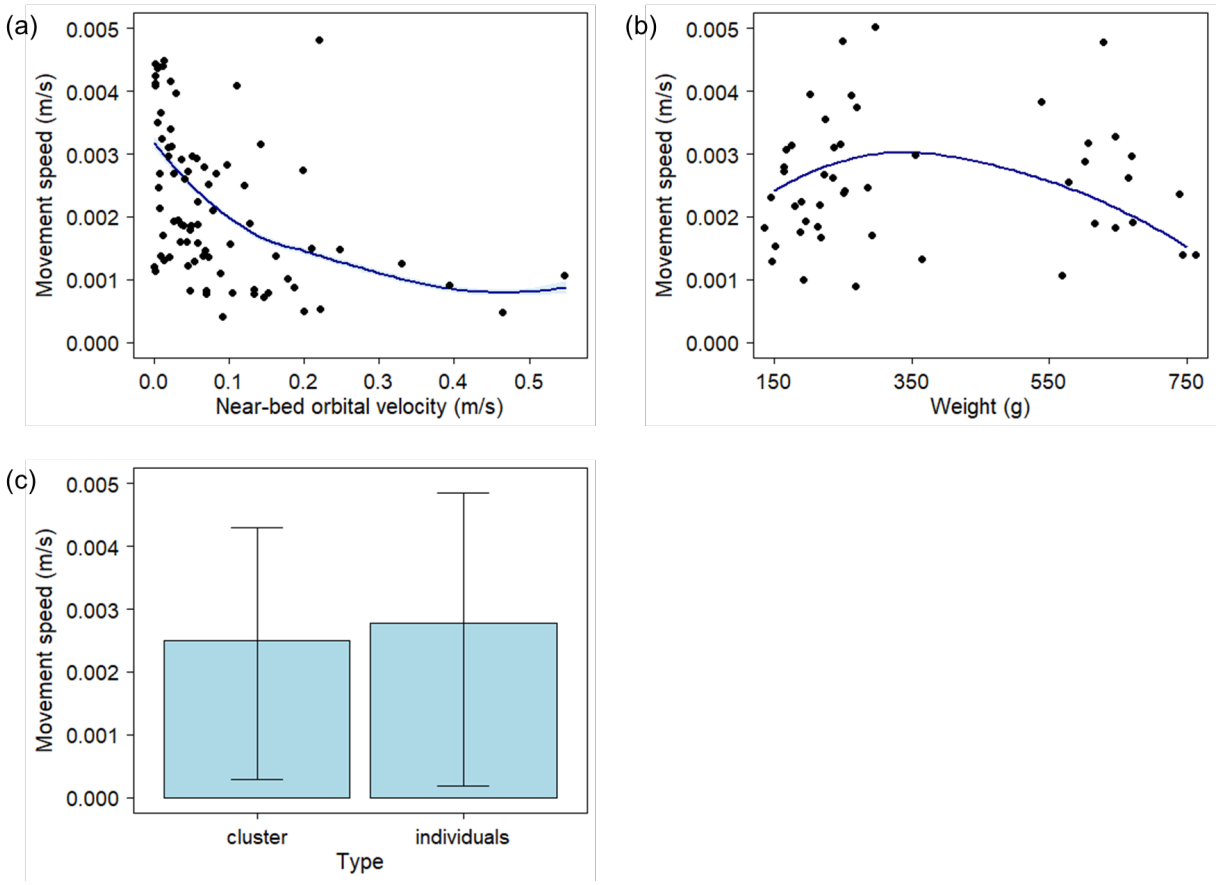

Fig. 4.10 Movement speed of flat oyster individuals and clusters in the study area as a function of near-bed velocity (a), weight (b) and type (c). Note that the slow movement here is presumed to be autonomous activity of oysters during their residency, as these movements occurred under calm hydrodynamic environments where the near-bed orbital velocity is far below the critical dislodgement threshold (i.e., 0.52 m s^{-1}) of flat oysters. In subplot a and b: the black scattered points are the statistical results of the measured data (i.e., the average speed at each velocity or weight); the dark blue curve is the fitting result of the GAMM (Generalized Additive Mixed Effects Model).

4.3.3 Activity space

The overall activity space (95% Kernel Utilization Distribution, KUD) of flat oyster individuals in the study area throughout the residency period ranged from 111 m^2 to 3279 m^2 (mean

= 1050 m^2). For flat oyster clusters, the overall activity space in the study area during the residency period ranged from 300 m^2 to 2692 m^2 (mean = 965 m^2).

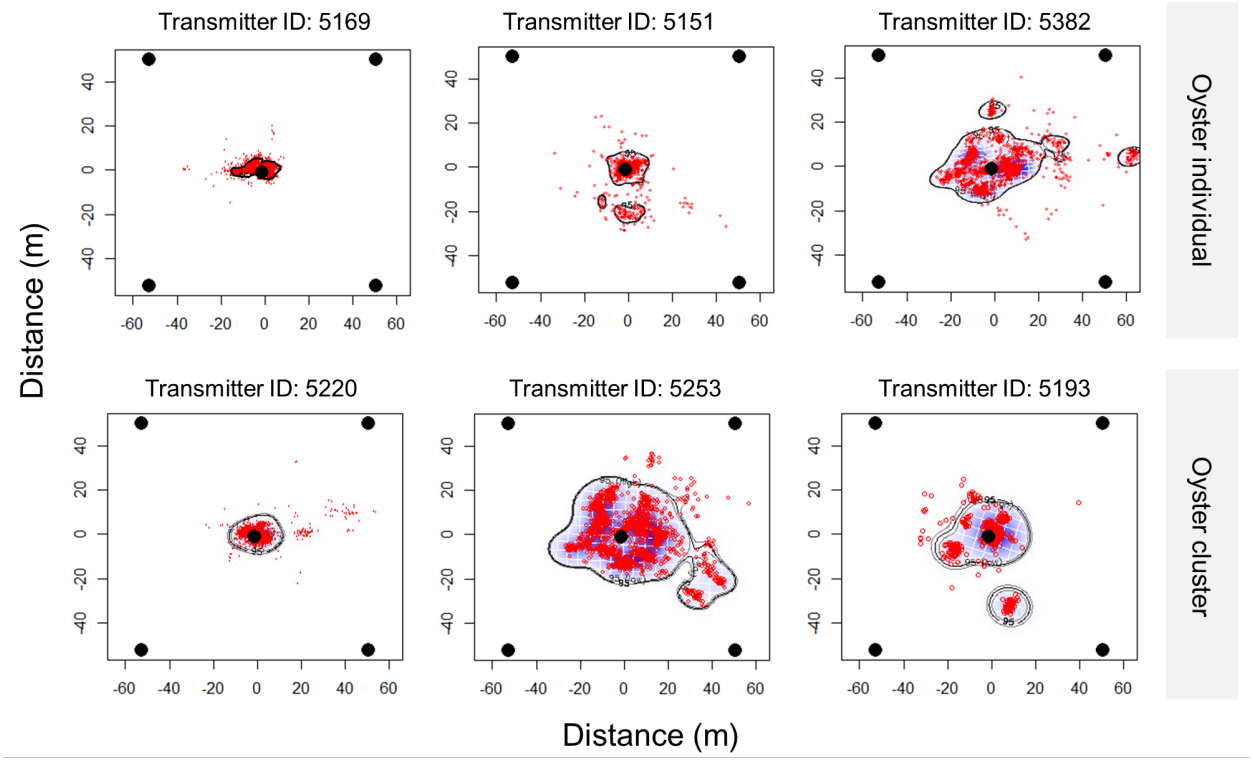

Fig. 4.11 Examples of the overall activity range (i.e., kernel utilization distribution; KUD) of flat oyster individuals and clusters throughout their residency period. The black dots represent the distribution of an acoustic telemetry array consisting of five receivers. The black circle indicates the activity range, and the red scatter points indicate the pinpoint positions. Darker blue within the black circle indicates higher kernel utilization.

GAMM results showed that weekly activity space of flat oyster individuals and clusters was not significantly affected by the type and near-bed orbital velocity (Fig. 4.12a, c), but was significantly affected by their weight (Table 4.2; Fig. 4.12b). Variability in activity range was more pronounced among oysters weighing between 150 and 350 g, with most of them corresponding to individual oysters. This showed a specific trend: smaller individuals typically move within a more confined spatial range, and this range tends to expand as their weight increases (Fig. 4.12b). However, larger weights (greater than 500 g; corresponding to oyster clusters) seem to limit the

expansion of the activity range, exhibiting a pattern similar to that of larger individual oysters but still greater than the activity range of smaller individual oysters (Fig. 4.12b).

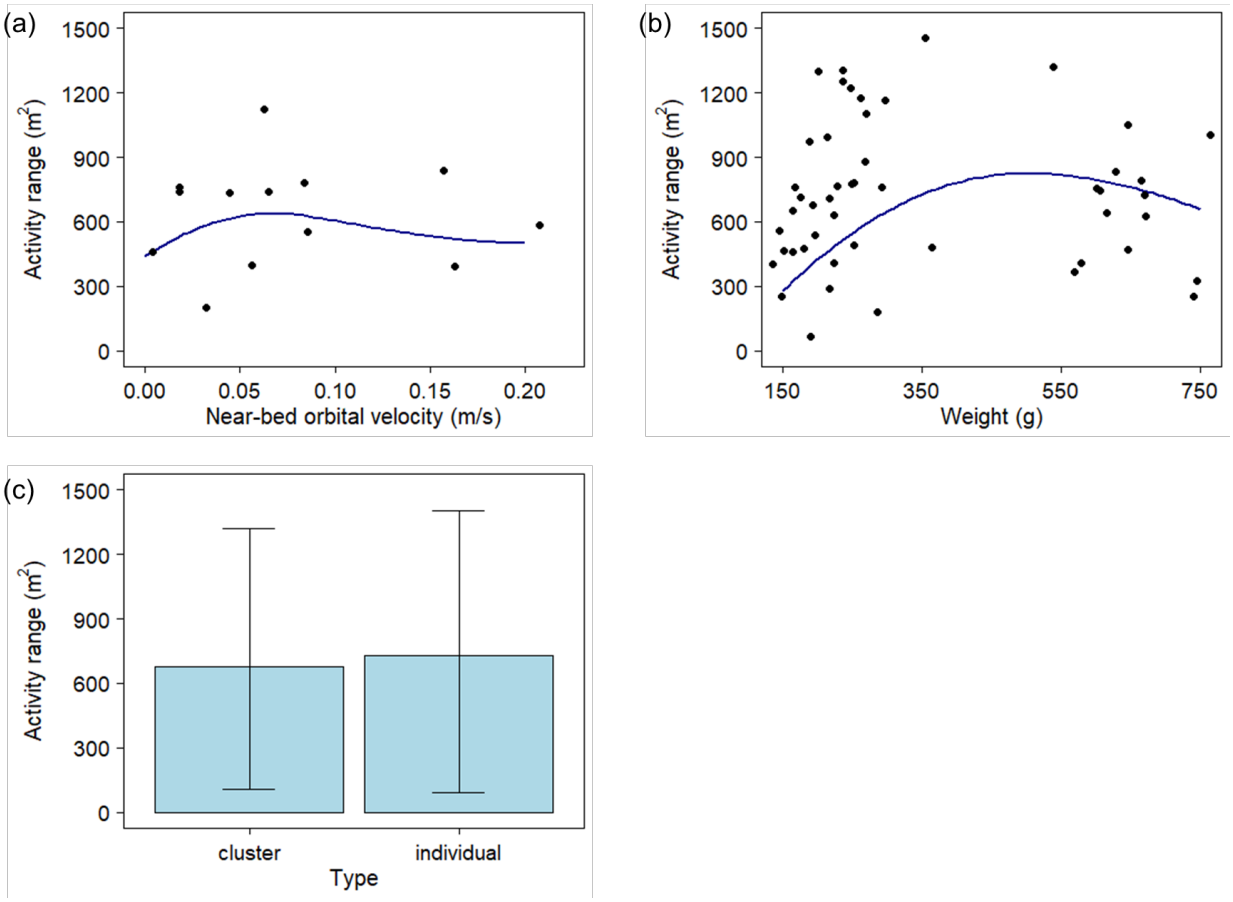

Fig. 4.12 Activity range of flat oyster individuals and clusters in the study area as a function of near-bed velocity (a), weight (b) and type (c). In subplot a and b: the black scattered points are the statistical results of the measured data (i.e., the average activity range at each velocity or weight); the dark blue curve is the fitting result of the GAMM (Generalized Additive Mixed Effects Model).

4.4 Discussion

In pursuit of research objective-3, we applied acoustic telemetry technology to monitor the performance of flat oyster restoration practices. This endeavor proved successful, as the method facilitated the pinpoint positioning of loosely deployed flat oysters with high temporal resolution, enabling us to reproduce their movement trajectories and activity range. Unfortunately, our results

indicated a significant displacement of deployed flat oysters during the restoration practice initiated in the winter of 2022 at the Gemini wind farm. Residency in the study area (i.e., within the acoustic telemetry array) was generally low, with the probability of presence mostly determined by local hydrodynamic regimes. Upon surpassing a specific hydrodynamic intensity, loosely deployed oyster individuals or clusters were expelled from the study area, validating the existence of a critical dislodgement threshold. It is worth noting that the critical dislodgement threshold inferred here using acoustic telemetry closely approximate that we quantified using accelerometers in Section-3. Furthermore, the persistent loss of signals within the acoustic telemetry array suggests that the expelled flat oysters did not return to the array but may instead be dispersed over a broader spatial range outside the research area.

Another possibility for the loss of acoustic telemetry signals is that the oysters, along with the transmitter, were buried by sediment (and shell materials). We did not include bed-level changes as a driving variable in the data analysis because 1) bed-level changes during the residence period of flat oysters were highly correlated with time; 2) this data was collected at a location 220 meters away from the study area and involved different substrates. Specifically, the substrate within the acoustic telemetry array consisted of shell materials, while the data collection site had a sandy substrate. The bed level of the latter tends to be more dynamic, as shells require higher shear stress to be lifted compared to sediments. Nevertheless, we could still discern patterns and make speculations from this data. Overall, the recorded bed levels were relatively stable (comparing to stormy years, such as 2021-2022; see Fig. 5.1) throughout the monitoring period, with some accretion (less than 10 cm) occurring in mid-January (Fig. 4.13). Subsequently, by late February, with the occurrence of erosion, the local bed level evolved back toward the initial bed level (Fig. 4.13). Although the loss of transmitter signals occurred at the end of January, if this were due to transmitters being buried, their signals should have been detected again following sediment erosion. In our case, this is not observed, leading us to strongly believe that the loss of telemetry signals is more likely due to the flat oysters being expelled from the study area by hydrodynamic forces rather than being buried by sediment.

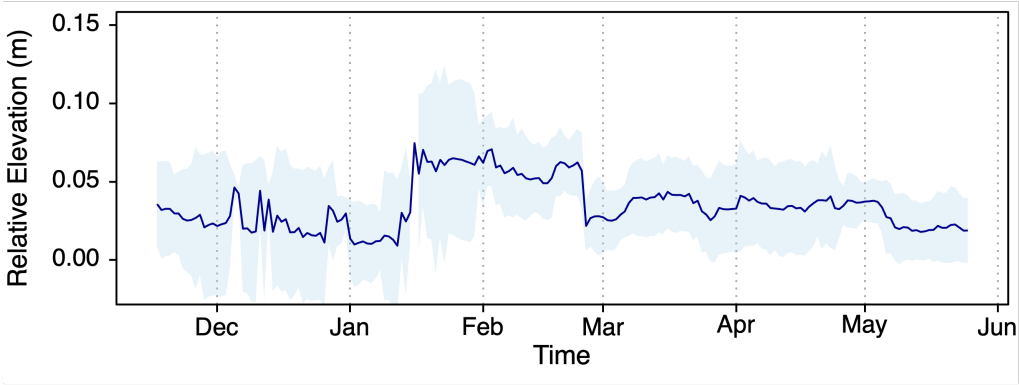

Fig. 4.13 Relative bed-level changes (i.e., relative elevation in Y-axis) recorded by ASED deployed on MIXLander during the winter of 2022-2023. Data are presented as daily averages. Positive values indicate accretion, and negative values indicate erosion.

During the residency of flat oysters, corresponding to periods of hydrodynamic calm, they do not remain stable in their initial settlement positions but continuously move within a certain range. In addition to the push from hydrodynamic forces (not powerful enough to cause oysters to be lost from the array), biological factors played an important role. Firstly, our GAMM results showed that the variability in activity range mainly existed among individual oysters. Specifically, larger individuals tend to move over a larger spatial range compared to smaller individuals. This is consistent with existing research, which demonstrated the importance of weight (or size) in the distribution of marine organisms (e.g., Papadopoulo et al., 2022). It is worth noting that as weight continues to increase, i.e., when oyster individuals attach to each other to form clusters, their activity space does not continue to expand. The largest oyster clusters involved in this study even exhibited a smaller activity range than larger oyster individuals. This suggests a non-linear trend in which the activity range may increase and then decrease with increasing weight. However, this study only considered individual oysters and clusters composed of three individuals, resulting in a polarization of the overall weight range, limiting a rigorous validation of this non-linear trend. Secondly, flat oysters exhibited extremely low movement speeds during residence, which were detected as being driven by near-bed velocity. Interestingly, faster movement of flat oysters occurred at lower near-bed orbital velocity, and they slowed down as near-bed orbital velocity increased (still below the critical dislodgement threshold of flat oysters). This implies that flat oysters adopt strategic adaptive behaviors under different hydrodynamic conditions (before the

critical dislodgement threshold is exceeded): moving under low-stress conditions and increasing their stability by reducing movement under high-stress conditions.

Overall, this study highlights that the primary challenge in restoration practices, particularly those involving the loose deployment of flat oysters, is the occurrence of high-energy hydrodynamic events. This emphasizes the urgent need to quantify the critical dislodgement threshold of flat oysters within the target restoration sites before initiating any restoration efforts.

5. General discussion

The central philosophy of restoring flat oyster reefs in the Dutch Wadden Sea is to kick-start a self-sustaining population (Sas et al., 2023), which typically entails two primary stages in current restoration pilots: (*i*) evaluating whether the conditions at the target sites are suitable to reintroduce and sustain flat oyster populations, and (*ii*) translocating adult oysters to re-establish a source of oyster larvae. This project developed the following monitoring approaches towards both stages:

- **Biophys sensor**: This sensor enables long-term, high-frequency, in-situ measurements of valve opening and closing in live oysters, making it an effective method for monitoring feeding behavior and health. The applicability of this sensor lies in evaluating whether the conditions at the target location support the healthy growth of flat oysters before and during restoration practices.
- **Biophy-logging package:** This package comprises flat oyster mimics equipped with accelerometers and a wave radar. Specifically, accelerometers were embedded in flat oyster shells to achieve long-term, high-frequency, in-situ monitoring of the stability of loosely deployed flat oysters (mimics). By integrating the high-frequency wave data obtained by the wave radar, this package enables the quantification of critical hydrodynamic thresholds that induce the dislodgement of loosely deployed flat oysters. This method is applicable for assessing whether the hydrodynamic conditions at the target location support the persistence of deployed flat oysters before and during restoration efforts.
- **Acoustic telemetry array**: This monitoring system relies on the detection of underwater acoustic signals to pinpoint the positions of loosely deployed flat oysters, allowing the reproduction of their long-term activity trajectories and ranges. This monitoring system should be applied concurrently with restoration practices, intuitively informing the success or failure of the restoration efforts and facilitating the identification of potential causes.

Based on the restoration practice implemented at the Gemini wind farm, these monitoring approaches were tested and applied to evaluate the performance of the restoration effort. Our monitoring results suggested:

1) The conditions within the Gemini wind farm meet the requirements for the healthy growth of flat oysters because our Biophys sensors detected the continuous valve opening and closing behavior of flat oysters, implying stable feeding and breathing. Temperature and salinity were identified as key factors and can be used as indicators to infer the habitat suitability regarding flat oyster feeding.
2) The critical dislodgement threshold for loosely deployed flat oysters within the Gemini wind farm has been successfully determined to be 0.52 m s^{-1}. This implies that once the local hydrodynamic intensity (i.e., near-bed orbital velocity) exceeds this threshold, flat oysters are at high risk of being expelled and carried along with the current. Comparing this threshold to changing hydrodynamic conditions will support the assessment and prediction of the long-term stability of flat oysters at the target location.
3) The flat oysters loosely deployed through the restoration practice within the Gemini wind farm have most likely moved far away from their initial deployment locations, as the acoustic telemetry array detected the complete loss of internally residing flat oysters within a short period (about two months). This was attributed to local hydrodynamic disturbances exceeding the critical dislodgement threshold of flat oysters on certain dates.

Most restoration pilots aimed to test factors such as survival, growth, and reproduction, as they are recognized as the most critical success factors once restoration efforts are launched in areas like the Dutch North Sea where flat oysters have disappeared (Schutter et al., 2021; Bos et al., 2023a; Sas et al., 2023). Biophys sensors can provide a cost-effective approach for this purpose. Relevant habitat suitability assessments have also been implemented in the Gemini wind farm. However, the findings of this project point to a fact: hydrodynamic-induced dislodgement formed the primary bottleneck for restoration efforts in which flat oysters (regardless of individuals and clusters) were loosely deployed. Despite the seawater conditions at the Gemini wind farm meeting the feeding needs of flat oysters (thus supporting their long-term healthy growth), hydrodynamic-induced dislodgement would cause the deployed flat oyster individuals and clusters to spread out over a larger spatial range, resulting in a sharp reduction in flat oyster density per unit area. In essence, a widely dispersed oyster population cannot serve as the starting point or incubator for a reef (Bos et al., 2023b). Therefore, future habitat suitability assessments for target restoration sites should give priority to local hydrodynamic regimes. This can be achieved by quantifying critical dislodgement thresholds for flat oyster individuals or clusters at target locations using our

developed Biophy-logging package, and then calculating return intervals for this threshold based on historical hydrodynamic records. In general, longer return intervals of the critical threshold suggest a lower likelihood of oyster dislodgement at that location.

It turns out that the restoration site involved in this project may not be an ideal location, as the critical dislodgement threshold of flat oysters was exceeded multiple times during the monitoring period, despite no officially named storms occurring. This implies that in years when storms occur (e.g., 2021-2022), restoration efforts through loosely deploying flat oyster individuals or clusters at that location will have a harder time maintaining stability. In line with the central philosophy of self-sustaining population restoration, employing artificial measures to enhance the stability of deployed flat oysters will be the last resort (Sas et al., 2023). A potential alternative strategy is to locate relatively hydrodynamically sheltered sites and deploy the initial populations there. The seabed within the Gemini wind farm may be dotted with relatively sheltered areas (e.g., channels between ridges and other types of depressions; van der Reijden et al., 2019) and/or areas with better settling substrate (e.g., high shelliness), making these locations more suitable for the formation/restoration of flat oyster reefs. To locate these areas, more extensive seabed surveys within the Gemini wind farm are necessary. Additionally, small rocks used as scour protection in the wind farm might serve as a combination of shelter and settling substrate (Kamermans et al., 2018; Tonk et al., 2020), but this requires rigorous on-site validation. In the innovative TreeReef project, an attempt was made to introduce shelter and settling substrate by using discarded pear trees. The pilot in the Dutch Wadden Sea demonstrated significant potential (Dickson, et al., 2023), but this option still needs further testing in offshore conditions.

Another significant challenge in flat oyster restoration is the unstable sediment regime (Housego et al., 2016; Sas et al., 2023). A substantial portion of the seabed within the Gemini wind farm is composed of sandy and silty sediments (Bruns et al., 2020), which could be suspended, dispersed, and resettled due to strong hydrodynamic disturbance (Gayer et al., 2006), potentially resulting in oysters being buried. This speculation is strongly supported by data obtained using ASED sensors in this project. Particularly in the winter of 2021-2022, four officially named storms (i.e., Corrie, Dudley, Eunice, and Franklin) occurred, leading to the accumulation of sediment deposition at the study area reaching up to 25 cm (Fig. 5.1). This depth of sediment accretion is sufficient to bury flat oyster individuals. However, the behavior of flat oysters in buried scenarios

remains unclear, posing unresolved questions: can flat oysters autonomously migrate to the sediment surface? How deep does sediment burial lead to the suffocation and mortality of flat oysters? These aspects need rigorous validation in future studies by employing controlled experiments. In contrast to the winter of 2021-2022, the sediment dynamics at the study area in the winter of 2022-2023 were relatively mild, with sediment accretion occurring from mid-January to the end of February, and subsequently returning to the initial bed level due to sediment erosion (Fig. 4.13). Despite the shallower burial, the impact of burial period on the behavior and health of flat oysters also requires further exploration. Additionally, a large amount of shell materials was lowered onto the seabed within the Gemini wind farm for substrate reconstruction during the restoration practice. This addition of shells materials was expected to provide attachment substrates for free-swimming oyster larvae (Tamburri et al., 2008; Colsoul et al., 2020). On the other hand, these shell materials may play a role in stabilizing local sediment, and the extent of their significance needs to be quantified in future practices using efficient approaches such as deploying ASED sensors.

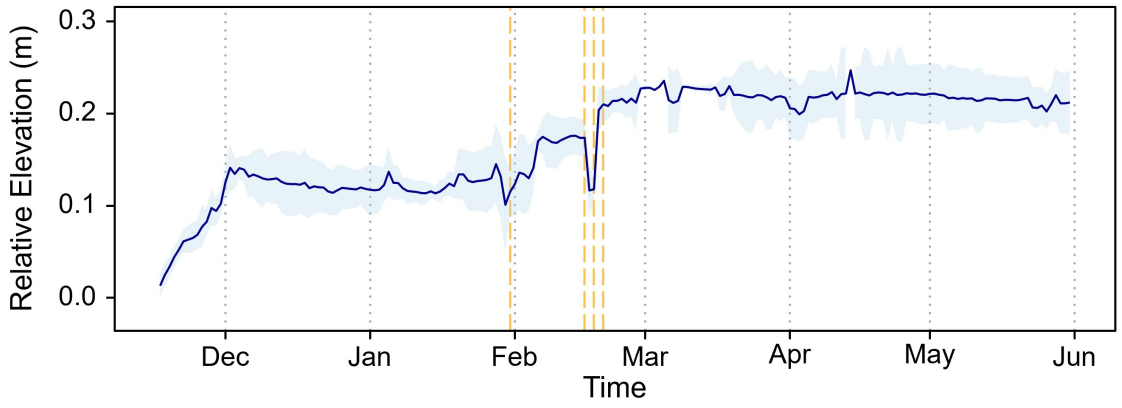

Fig. 5.1 Relative bed-level changes (i.e., relative elevation in the Y-axis) recorded by ASED deployed on MIXLander during the winter of 2021-2022. Refer to section 2.2.2 for details about MIXLander, and section 4.2.3 for information on how the ASED works. Data are presented as daily averages, with positive values indicating accretion and negative values indicating erosion. The dashed orange lines represent the dates of the storms, including Corrie (January 31, 2022), Dudley (February 16, 2022), Eunice (February 18, 2022), and Franklin (February 20, 2022).

6. References

Baggett, L. P., Powers, S. P., Brumbaugh, R. D., Coen, L. D., DeAngelis, B. M., Greene, J. K., Hancock, B. T., Morlock, S. M., Allen, B. L., Breitburg, D. L., Bushek, D., Grabowski, J. H., Grizzle, R. E., Grosholz, E. D., La Peyre, M. K., Luckenbach, M. W., McGraw, K. A., Piehler, M. F., Westby, S. R., & Zu Ermgassen, P. S. (2015). Guidelines for evaluating performance of oyster habitat restoration. Restoration Ecology, 23(6), 737-745.

Bennema, F. P., Engelhard, G. H., & Lindeboom, H. (2020). *Ostrea edulis* beds in the central North Sea: delineation, ecology, and restoration. ICES Journal of Marine Science, 77(7-8), 2694-2705.

Bertolini, C., Capelle, J., Royer, E., Milan, M., Witbaard, R., Bouma, T. J., & Pastres, R. (2022). Using a clustering algorithm to identify patterns of valve-gaping behaviour in mussels reared under different environmental conditions. Ecological Informatics, 69, 101659.

Bos, O. G., Duarte-Pedrosa, S., Didderen, K., Bergsma, J. H., Heye, S., & Kamermans, P. (2023a). Performance of European oysters (*Ostrea edulis* L.) in the Dutch North Sea, across five restoration pilots. Frontiers in Marine Science, 10.

Bos, O. G., Kamermans, P., Tonk, L., Schutter, M., Maathuis, M., van Gool, A., van der Have, T., Bergsma, J., Raaijmakers, T., van Duren, L., Emmanouil, A., Gerritsma, I., Kleissen, F., & Sas, H. (2023b). Eco-friendly reef restoration pilots in offshore wind farms: Report Project ECOFRIEND 2019-2023 (No. C018/23). Wageningen Marine Research.

Bruns, I., Holler, P., Capperucci, R. M., Papenmeier, S., & Bartholomä, A. (2020). Identifying trawl marks in north sea sediments. Geosciences, 10(11), 422.

Colden, A. M., Fall, K. A., Cartwright, G. M., & Friedrichs, C. T. (2016). Sediment suspension and deposition across restored oyster reefs of varying orientation to flow: implications for restoration. Estuaries and Coasts, 39, 1435-1448.

Colsoul, B., Pouvreau, S., Di Poi, C., Pouil, S., Merk, V., Peter, C., Boersma, M., & Pogoda, B. (2020). Addressing critical limitations of oyster (*Ostrea edulis*) restoration: Identification

of nature‐based substrates for hatchery production and recruitment in the field. Aquatic Conservation: Marine and Freshwater Ecosystems, 30(11), 2101-2115.

Crawford, C., Edgar, G., Gillies, C. L., & Heller-Wagner, G. (2019). Relationship of biological communities to habitat structure on the largest remnant flat oyster reef (*Ostrea angasi*) in Australia. Marine and Freshwater Research, 71(8), 972-983.

Didderen, K., Lengkeek, W., Bergsma, J. H., van Dongen, U., Driessen, F. M. F., & Kamermans, P. (2020). WWF & ARK Borkum Reef Ground oyster pilot: Active restoration of native oysters in the North Sea-Monitoring September 2019 (No. 19-227). Bureau Waardenburg.

Dickson, J., Franken, O., Watson, M. S., Monnich, B., Holthuijsen, S., Eriksson, B. K., Govers, L., van der Heide, T., & Bouma, T. J. (2023). Who lives in a pear tree under the sea? A first look at tree reefs as a complex natural biodegradable structure to enhance biodiversity in marine systems. Frontiers in Marine Science, 10, 1213790.

Didderen, K., Bergsma, J. H., & Kamermans, P. (2019). Offshore flat oyster pilot Luchterduinen wind farm: Results campaign 2 (July 2019) and lessons learned (No. Report no. 19-184). Bureau Waardenburg.

Esagholian Khoygane, S. (2021). Methods for studying coastal bivalves in a changing world: A review and implications for management (Master thesis, University of Agder).

Espinoza, M., Farrugia, T. J., & Lowe, C. G. (2011). Habitat use, movements and site fidelity of the gray smooth-hound shark (*Mustelus californicus* Gill 1863) in a newly restored southern California estuary. Journal of Experimental Marine Biology and Ecology, 401(1-2), 63-74.

Fowler, A. M., Jørgensen, A. M., Coolen, J. W., Jones, D. O., Svendsen, J. C., Brabant, R., Rumes, B., & Degraer, S. (2020). The ecology of infrastructure decommissioning in the North Sea: what we need to know and how to achieve it. ICES Journal of Marine Science, 77(3), 1109-1126.

Gayer, G., Dick, S., Pleskachevsky, A., & Rosenthal, W. (2006). Numerical modeling of suspended matter transport in the North Sea. Ocean dynamics, 56, 62-77.

Gercken, J., & Schmidt, A. (2014). Current status of the European Oyster (*Ostrea edulis*) and possibilities for restoration in the German North Sea. Bundesamt für Naturschutz.

Hays, G. C., Mortimer, J. A., Rattray, A., Shimada, T., & Esteban, N. (2021). High accuracy tracking reveals how small conservation areas can protect marine megafauna. Ecological Applications, 31(7), e02418.

Hermans, A., Bos, O. G., & Prusina, I. (2020). Nature-Inclusive Design: a catalogue for offshore wind infrastructure: Technical report (No. 114266/20-004.274).

Housego, R. M., & Rosman, J. H. (2016). A model for understanding the effects of sediment dynamics on oyster reef development. Estuaries and Coasts, 39(2), 495-509.

Kamermans, P., Walles, B., Kraan, M., Van Duren, L. A., Kleissen, F., Van der Have, T. M., Smaal, A. C., & Poelman, M. (2018). Offshore wind farms as potential locations for flat oyster (*Ostrea edulis*) restoration in the Dutch North Sea. Sustainability, 10, 308.

Kerckhof, F., Coolen, J. W., Rumes, B., & Degraer, S. (2018). Recent findings of wild European flat oysters *Ostrea edulis* (Linnaeus, 1758) in Belgian and Dutch offshore waters: new perspectives for offshore oyster reef restoration in the southern North Sea. Belgian Journal of Zoology, 148(1).

Kreeger, D. A., Gatenby, C. M., & Bergstrom, P. W. (2018). Restoration potential of several native species of bivalve molluscs for water quality improvement in mid-Atlantic watersheds. Journal of Shellfish Research, 37(5), 1121-1157.

Lennox, R. J., Aarestrup, K., Alós, J., Arlinghaus, R., Aspillaga, E., Bertram, M. G., Birnie-Gauvin, K., Brodin, T., Cooke, S. J., Dahlmo, L. S., Dhellemmes, F., Gjelland, K., Hellström, G., Hershey, H., Holbrook, C., Klefoth, T., Lowerre-Barbieri, S., Monk, C. T., Nilsen, C. I., Pauwels, I., Pickholtz, R., Prchalová, M., Reubens, J., Říha, M., Villegas-Ríos, D., Vollset, K. W., Westrelin, S., & Baktoft, H. (2023). Positioning aquatic animals with acoustic transmitters. Methods in Ecology and Evolution, 14(10), 2514-2530.

Luff, R., & Moll, A. (2004). Seasonal dynamics of the North Sea sediments using a three-dimensional coupled sediment–water model system. Continental Shelf Research, 24(10), 1099-1127.

Merk, V., Colsoul, B., & Pogoda, B. (2020). Return of the native: survival, growth and condition of European oysters reintroduced to German offshore waters. Aquatic Conservation: Marine and Freshwater Ecosystems, 30(11), 2180-2190.

OFL (2020). Het Akkoord voor de Noordzee, Overlegorgaan Fysieke Leefomgeving, 2020.

Papadopoulo, K., Villegas-Ríos, D., Mucientes, G., Hillinger, A., & Alonso-Fernández, A. (2023). Drivers of behaviour and spatial ecology of the small spotted catshark (*Scyliorhinus canicula*). Aquatic Conservation: Marine and Freshwater Ecosystems.

Plunket, J., & La Peyre, M. K. (2005). Oyster beds as fish and macroinvertebrate habitat in Barataria Bay, Louisiana. Bulletin of Marine Science, 77(1), 155-164.

Pineda-Metz, S. E., Colsoul, B., Niewöhner, M., Hausen, T., Peter, C., & Pogoda, B. (2023). Setting the stones to restore and monitor European flat oyster reefs in the German North Sea. Aquatic Conservation: Marine and Freshwater Ecosystems.

Pogoda, B. (2019). Current status of European oyster decline and restoration in Germany. Humanities, 8(1), 9.

Sas, H., van Duren, L., Herman, P. M., van der Have, T., Kamermans, P., Bos, O. G., Kingma, E., Bouma, T. J., & Kardinaal, E. (2023). Reef-building species and biogenic reef enhancement in the Dutch North Sea: Background documents.

Schutter, M., Tonk, L., Kamermans, P., Kardinaal, E., & ter Hofstede, R. (2021). EcoScour project Borssele V− Outplacement methods of European flat oysters. Report Bureau Waardenburg, 21-328.

Smaal A., Kamermans P., van der Have T. M., Engelsma M., Sas H. J. W. (2015). Feasibility of Flat Oyster (*Ostrea edulis* L.) restoration in the Dutch part of the North Sea. Report C028/15 (IMARES Wageningen UR).

Smaal, A., Kamermans, P., Kleissen, F., van Duren, L., & van der Have, T. (2017). Flat oysters on offshore wind farms: opportunities for the development of flat oyster populations on existing and planned wind farms in the Dutch section of the North Sea (No. C052/17). Wageningen Marine Research.

Smith, D. M., & Murphy, J. M. (2007). An objective ocean temperature and salinity analysis using covariances from a global climate model. Journal of Geophysical Research: Oceans, 112(C2).

Stechele, B., Barbut, L., Lacroix, G., van Duren, L. A., Van Lancker, V., Degraer, S., Gavazzi, G. M., Bossier, P., Declercq, A. M., & Nevejan, N. (2023a). Northern Europe's suitability for offshore European flat oyster (*Ostrea edulis*) habitat restoration based on population dynamics. Frontiers in Marine Science, 10.

Stechele, B., Hughes, A., Degraer, S., Bossier, P., & Nevejan, N. (2023b). Northern Europe's suitability for offshore European flat oyster (*Ostrea edulis*) habitat restoration: A mechanistic niche modelling approach. Aquatic Conservation: Marine and Freshwater Ecosystems.

Tamburri, M. N., Luckenbach, M. W., Breitburg, D. L., & Bonniwell, S. M. (2008). Settlement of Crassostrea ariakensis larvae: effects of substrate, biofilms, sediment and adult chemical cues. Journal of Shellfish Research, 27(3), 601-608.

Tonk, L., Witte, S., & Kamermans, P. (2020). Flat oyster (*Ostrea edulis*) settlement on scour protection material: Innovation Eco Scour Protection in offshore windfarm Borssele V (No. C063/20). Wageningen Marine Research.

Tonk, L., Witbaard, R., van Dalen, P., Cheng, C. H., & Kamermans, P. (2023). Applicability of the gape monitor to study flat oyster (*Ostrea edulis*) feeding behaviour. Aquatic Living Resources, 36(6).

Tsujino, H., Urakawa, L. S., Griffies, S. M., Danabasoglu, G., Adcroft, A. J., Amaral, A. E., & Yu, Z. (2020). Evaluation of global ocean–sea-ice model simulations based on the experimental protocols of the Ocean Model Intercomparison Project phase 2 (OMIP-2). Geoscientific Model Development, 13(8), 3643-3708.

van Der Reijden, K. J., Koop, L., O'flynn, S., Garcia, S., Bos, O., van Sluis, C., Maaholm, D. J., Herman, M. J., Simons, D. G., Olff, H., Ysebaert, T., Snellen, M., Govers, L. L., Rijnsdorp, A. D., & Aguilar, R. (2019). Discovery of Sabellaria spinulosa reefs in an intensively fished area of the Dutch Continental Shelf, North Sea. Journal of Sea Research, 144, 85-94.

van Duren, L., Kamermans, P., & Kleissen, F. (2022). Suitability for the development of flat oyster populations in new offshore wind farm zones and two search areas for restoration projects in the Dutch section of the North Sea (No. 11208312-002-ZKS-0001). Deltares.

Zamora, L., & Moreno-Amich, R. (2002). Quantifying the activity and movement of perch in a temperate lake by integrating acoustic telemetry and a geographic information system. In Aquatic Telemetry: Proceedings of the Fourth Conference on Fish Telemetry in Europe (pp. 209-218). Springer Netherlands.

Zu Ermgassen, P. S., Bos, O. G., Debney, A., Gamble, C., Glover, A., Pogoda, B., Pouvreau, S., Sanderson, W., Smyth, D., & Preston, J. (2021). European native oyster habitat restoration monitoring handbook. The Zoological Society of London.